

Dihydrothiazolopyridone Derivatives as a Novel Family of Positive Allosteric Modulators of the Metabotropic Glutamate 5 (mGlu₅) Receptor

José Manuel Bartolomé-Nebreda,^{*,†} Susana Conde-Ceide,[†] Francisca Delgado,[†] Laura Iturrino,[¶] Joaquín Pastor,[†] Miguel Ángel Pena,[†] Andrés A. Trabanco,[†] Gary Tresadern,[‡] Carola M. Wassvik,[‡] Shaun R. Stauffer,^{§,||,⊥,♯} Satyawar Jadhav,^{§,||} Kiran Gogi,^{§,||} Paige N. Vinson,^{§,||} Meredith J. Noetzel,^{§,||} Emily Days,^{§,Δ} C. David Weaver,^{§,Δ} Craig W. Lindsley,^{§,||,⊥,♯} Colleen M. Niswender,^{§,||,⊥} Carrie K. Jones,^{§,||,⊥} P. Jeffrey Conn,^{§,||,⊥} Frederik Rombouts,[○] Hilde Lavreysen,[●] Gregor J. Macdonald,[○] Claire Mackie,[▲] and Thomas Steckler[●]

[†]Neuroscience Medicinal Chemistry, [¶]CREATE Analytical Sciences, and [‡]CREATE Molecular Informatics, Janssen Research and Development, Jarama 75, 45007 Toledo, Spain

[§]Department of Pharmacology and ^{||}Vanderbilt Center for Neuroscience Drug Discovery, Vanderbilt University Medical Center, Nashville, Tennessee 37232, United States

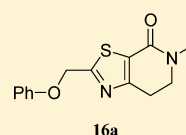
[⊥]Vanderbilt Specialized Chemistry Center for Probe Development (MLPCN), Nashville, Tennessee 37232, United States

[♯]Department of Chemistry and ^ΔVanderbilt Institute of Chemical Biology, Vanderbilt University, Nashville, Tennessee 37232, United States

[○]Neuroscience Medicinal Chemistry, [●]Neuroscience Biology, and [▲]CREATE Discovery ADME/Tox, Janssen Research and Development, Turnhoutseweg 30, B-2340, Beerse, Belgium

S Supporting Information

ABSTRACT: Starting from a singleton chromanone high throughput screening (HTS) hit, we describe a focused medicinal chemistry optimization effort leading to the identification of a novel series of phenoxymethyl-dihydrothiazolopyridone derivatives as selective positive allosteric modulators (PAMs) of the metabotropic glutamate 5 (mGlu₅) receptor. These dihydrothiazolopyridones potentiate receptor responses in recombinant systems. In vitro and in vivo drug metabolism and pharmacokinetic (DMPK) evaluation allowed us to select compound **16a** for its assessment in a preclinical animal screen of possible antipsychotic activity. **16a** was able to reverse amphetamine-induced hyperlocomotion in rats in a dose-dependent manner without showing any significant motor impairment or overt neurological side effects at comparable doses. Evolution of our medicinal chemistry program, structure activity, and properties relationships (SAR and SPR) analysis as well as a detailed profile for optimized mGlu₅ receptor PAM **16a** are described.



hmGlu₅ EC₅₀ = 1195 nM, 89% Glu Max
rmGlu₅ EC₅₀ = 3408 nM, 62% Glu Max
mGlu_{1,4,6-8} > 10 μM
Glutamate Fold Shift (h) = 4.4 (10 μM)
Kinetic solubility (pH 7.4) = 97 μM
LM (h, r) = 22, 68% metabolized after 15 min

INTRODUCTION

Schizophrenia is a mental disorder that affects approximately 1% of the world population.¹ This severely limiting illness is characterized by a combination of so-called positive (e.g., hallucinations and delusions), negative (e.g., anhedonia and poverty of speech), and cognitive symptoms.¹ Currently available therapies, “typical” and “atypical” antipsychotics, rely on dopamine 2 (D₂) receptor antagonism to exert their action, and, despite being highly efficacious in addressing positive symptoms, they are of limited value for the treatment of the other core symptoms of the disease. Furthermore, their clinical use is associated with a plethora of severe side-effects (e.g., Parkinson-like extrapyramidal symptoms (EPS), prolactin release, weight gain, or cardiac risk), and as such, patient compliance is extremely poor. As a result, during the past 10–15 years, several alternative mechanisms of action that do not

involve direct interaction with dopaminergic receptors have been proposed and investigated.^{2,3} The ultimate hope is that different biological pathways may lead to effective antipsychotic medications with both increased efficacy versus all three core symptom domains and improved tolerability due to the lack of direct D₂ receptor blockade.

One of the proposed pathophysiological causes that may lead to schizophrenia is a compromised function of *N*-methyl-D-aspartate (NMDA) receptors. This NMDA receptor hypofunction triggers a cascade of events, i.e., reduced activation of inhibitory γ-aminobutyric acidergic (GABAergic) interneurons in thalamus and cortex with a consequent disinhibition of excitatory glutamatergic pathways.⁴ On the basis of these

Received: May 2, 2013

Published: August 15, 2013

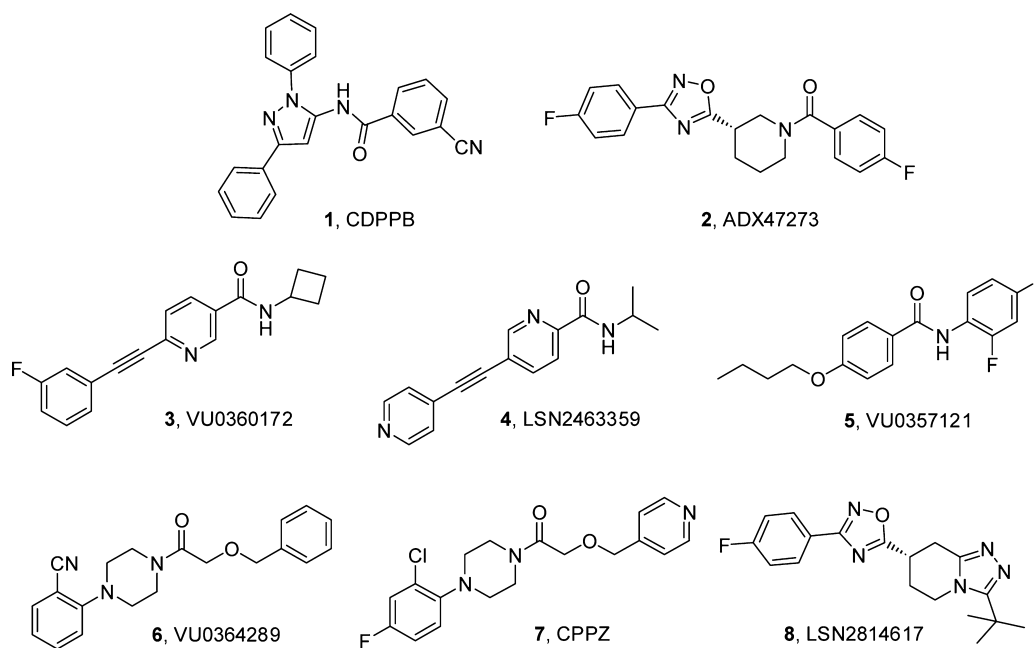


Figure 1. mGlu₅ receptor PAMs with reported efficacy in preclinical models of schizophrenia and cognition.

observations, it has been proposed that compounds that enhance NMDA receptor function may have beneficial effects in schizophrenia. Unfortunately, direct agonists of the NMDA receptor tend to be neurotoxic; hence, alternative strategies to increase NMDA receptor function have been suggested. A desired increase in NMDA receptor function may be obtained through an indirect modulation of NMDA receptors via metabotropic glutamate (mGlu) receptors, especially mGlu₅ receptors.² The mGlu₅ receptor belongs to the Group I mGlu receptor subfamily, together with the mGlu₁ receptor.⁵ They activate phospholipase C (PLC) via coupling to G_q proteins and are ubiquitously expressed on postsynaptic excitatory terminals in limbic brain regions that are involved in motivational, emotional, and cognitive processes.⁶ At GABA-ergic interneurons, mGlu₅ and NMDA receptors are coexpressed⁷ and are not only coupled via intracellular signaling pathways but also physically through scaffolding proteins.⁸ In summary, mGlu₅ receptor-mediated activation of NMDA receptor functioning has recently emerged as a promising non-dopamine based approach for potential therapeutic intervention of schizophrenia.²

Taking into account the challenges associated with the development of orthosteric agonists for mGlu receptors (e.g., poor druglike properties, elusive selectivity, or potential tolerance development), current strategies have mainly focused on the identification of positive allosteric modulators (PAMs).⁹ This approach has already proven useful, and in vivo activity in different preclinical schizophrenia and cognition models has been reported for early prototypical mGlu₅ PAMs such as 3-cyano-*N*-(1,3-diphenyl-1*H*-pyrazol-5-yl)benzamide (CDPPB, **1**)^{10,11} or *S*-(4-fluoro-phenyl)-{3-[3-(4-fluoro-phenyl)-[1,2,4]-oxadiazol-5-yl]-piperidin-1-yl}-methanone (ADX47273, **2**)¹² and more recently for novel structurally distinct chemical series including *N*-cyclobutyl-6-((3-fluorophenyl)ethynyl)-nicotinamide (VU0360172, **3**),¹³ *N*-(1-methylethyl)-5-(pyridin-4-ylethynyl)pyridine-2-carboxamide (LSN2463359, **4**),^{14,15} 4-butoxy-*N*-(2,4-difluorophenyl)benzamide (VU0357121, **5**),¹⁶ 2-(4-(2-(benzyloxy)acetyl)piperazin-1-yl)benzonitrile

(VU0364289, **6**),¹⁷ 1-(4-(2-chloro-4-fluorophenyl)piperazin-1-yl)-2-(pyridin-4-ylmethoxy)ethanone (CPPZ, **7**),¹⁸ and (7*S*)-3-*tert*-butyl-7-[3-(4-fluorophenyl)-1,2,4-oxadiazol-5-yl]-5,6,7,8-tetrahydro[1,2,4]triazolo[4,3-*a*]pyridine (LSN2814617, **8**).¹⁵ These novel PAM classes represent a significant evolution from the first generation as they offer improved drug-likeness (e.g., improved solubility, unbound fraction in brain or oral bioavailability and in vivo efficacy). Although the preclinical biological data clearly suggest the potential of mGlu₅ receptor PAMs as a novel class of antipsychotic agents, the identification of a compound suitable for clinical proof-of-concept studies still remains a challenge and will be crucial to clarify the potential role of mGlu₅ receptor PAMs as improved antipsychotics.

RESULTS

Given the promise offered by mGlu₅ receptor PAMs as a potential novel treatment for schizophrenia, we performed an HTS campaign looking for starting points for a medicinal chemistry program. The in vitro mGlu₅ PAM calcium mobilization assay provides two measures of compound activity: pEC₅₀, which is defined as the negative logarithm of the concentration at which half-maximal potentiation of glutamate is reached, and the maximal increase in observed glutamate response, the % Glu Max. Screening of the Janssen corporate library in a cell line expressing the human mGlu₅ receptor with this functional calcium mobilization assay resulted in the identification of the subsequently reported chromanone **9**,¹⁹ as a promising hit. Compound **9** possessed potent in vitro mGlu₅ PAM activity (EC₅₀ = 128 nM, Glu Max = 82%). As a first step, and since molecule **9** contains labile substructures such as the ester group, we verified that the products of the ester hydrolysis, benzoic acid and 6-hydroxy-chromanone, were not responsible for the mGlu₅ PAM activity of the HTS sample of **9**. Both compounds were found to be inactive under the same assay conditions (EC₅₀ > 10 μM), while quality control of the sample **9** was good (LCMS purity > 95%), providing confidence in the HTS in vitro data. Furthermore, **9** showed satisfactory selectivity²⁰ versus other

representative members of the mGlu family (mGlu_{1,2,8} EC₅₀ > 10 μ M). Unfortunately, and as anticipated from the presence of the carboxylic ester functionality, **9** was found to be completely hydrolyzed in rat plasma, which precluded any further work for its in vivo pharmacological characterization. Nevertheless, compound **9** was considered as a good starting point for optimization due to its low molecular weight, moderate lipophilicity (clogP = 3.3), high ligand efficiency²¹ (LE = 0.34), and promising selectivity.

As seen in Figure 2, our strategy for the exploration of the chromanone **9** followed two parallel approaches, first fixing the

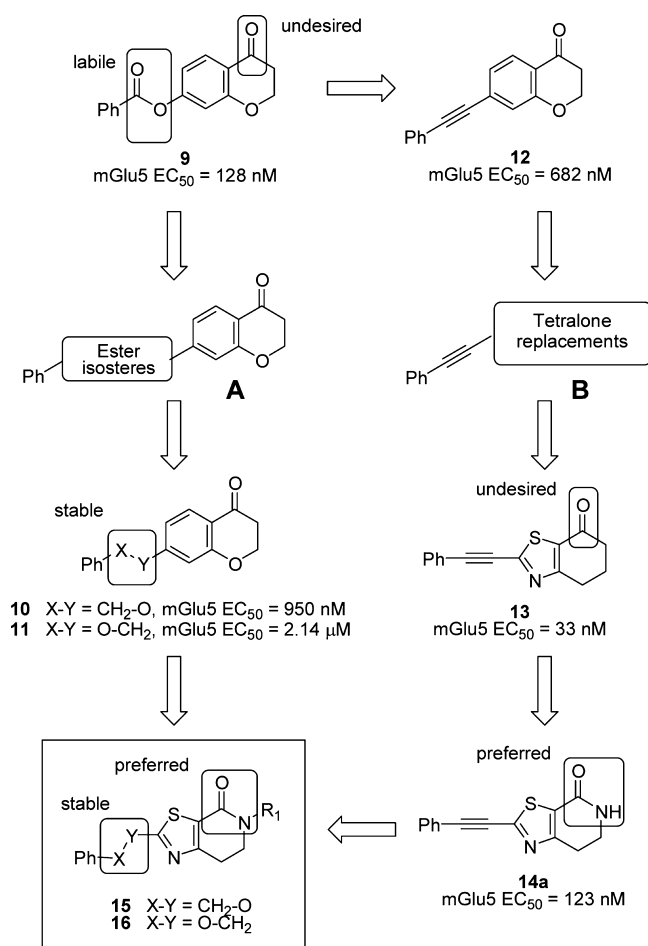


Figure 2. Parallel simultaneous evolution from HTS hit **9** to optimized series **15** and **16**.

chromanone scaffold while performing an extensive search for replacements for the labile ester group (A) and, in addition, seeking to replace and optimize the chromanone bicycle as it also contains a ketone moiety, a potential metabolic hot spot and biologically reactive group (B).

Approach A involved the synthesis and evaluation of several libraries of diverse potential ester surrogates including, among others, alkyls, amides, amines, heterocycles, and ethers as alternate spacers between the chromanone core and the distal phenyl ring.²² Among this set of linkers, only previously published benzyloxy and phenoxyethyl derivatives **10** and **11**¹⁹ retained significant mGlu₅ receptor PAM activity (EC₅₀ = 950 nM, 76% Glu Max and EC₅₀ = 2.14 μ M, 94% Glu Max respectively) and promising selectivity versus the other mGlu receptor subtypes (mGlu_{1-4,6-8} EC₅₀ > 10 μ M). Similar

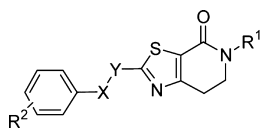
moieties have recently been reported for other mGlu₅ PAM chemotypes.^{19,23}

For the second prong of our strategy, chromanone replacements were sought using different approaches. It is now becoming clear in the literature that some of the most potent in vitro mGlu₅ receptor PAMs have a common phenylacetylene moiety.⁹ For comparative purposes, we synthesized the corresponding phenylacetylene chromanone analogue **12**¹⁹ which was also found to be an mGlu₅ receptor PAM (EC₅₀ = 682 nM, Glu Max 84%) although with an approximately 5-fold decrease in activity compared to the initial HTS hit **9**. Following this result, we decided to keep the acetylenic spacer constant and combine it with different bicyclic systems with the underlying rationale that this could increase the ability to sample and identify chromanone alternatives. To prioritize among the multiple existing possibilities, our design principle focused on bicyclic scaffolds possessing hydrogen bond acceptors that could mimic those present in the chromanone core. This strategy proved fruitful as among the initial set of compounds synthesized, dihydrobenzothiazolone derivative **13**²⁴ emerged as a highly potent (~21 fold potency increase vs **12**), efficacious and selective mGlu₅ receptor PAM (EC₅₀ = 33 nM, 71% Glu Max, mGlu_{1-4,6-8} > 10 μ M). Despite its high potency and promising metabolic stability in human liver microsomes (55% remaining after 15 min incubation), **13** was found to be highly unstable in rat liver microsomes (2% remaining after 15 min incubation), likely due to the presence of the exposed keto-group. Furthermore, **13** was poorly soluble in aqueous buffer (30 μ M, pH 7.4), and it could not be formulated in our standard carrier for in vivo testing [<0.25 mg/mL in 20% hydroxypropyl- β -cyclodextrin (HP- β -CD) formulation in water]. Therefore, we focused efforts on the identification of metabolically stable analogues of **13** bearing a carbonyl function less prone to metabolism. For this purpose, we considered the conversion of the dihydrobenzothiazolone of **13** into a dihydrothiazolopyridone scaffold. Despite an approximate 4-fold decrease in potency with respect to **13**, compound **14a** showed comparable mGlu₅ potency (EC₅₀ = 123 nM, 79% Glu Max) to HTS hit **9**. In addition, **14a** was selective versus the other mGlu receptors at the screening concentration of 10 μ M. Importantly, **14a** showed a remarkably reduced turnover in both human and rat liver microsomes (85% and 63% respectively remaining after 15 min incubation at 1 μ M concentration). Furthermore, the amide functionality present in the dihydrothiazolopyridone core of **14a** represents an attractive chemical handle amenable for further derivatization for structure-activity relationship (SAR) expansion purposes. A preliminary evaluation of tertiary amides showed that the introduction of alkyl substituents could lead to a comparable activity in the case of the methyl derivative **14b** (EC₅₀ = 193 nM, 57% Glu Max) or the methoxyethyl substituted example **14c** (EC₅₀ = 119 nM, 47% Glu Max) although with a drop of Glu Max in both examples.

At this point, having accomplished our initial goal of identifying separate replacements for the ester and keto functions, we decided to combine both approaches and target the synthesis of the corresponding series of benzyloxy- and phenoxyethyl-dihydrothiazolopyridone combinations **15** and **16**, respectively (Table 1).²⁵

Chemistry. Compound **13** was readily prepared in two steps (39% overall yield), via Sandmeyer reaction and subsequent Sonogashira cross-coupling, from 2-amino-benzothiazolone **17**²⁶ (Scheme 1).

Table 1. Structures and Activities of Substituted Benzyloxy- and Phenoxyethyl-dihydrothiazolopyridones 15 and 16




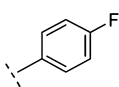

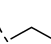
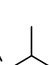
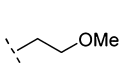
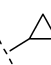
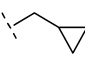
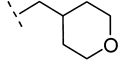
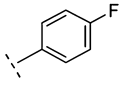
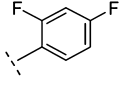
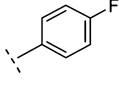
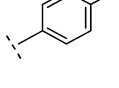
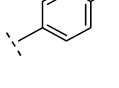
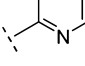
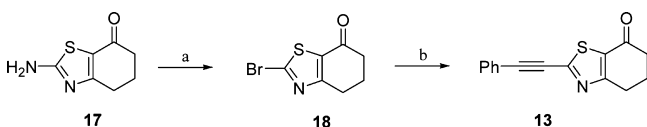
Comp	X-Y	R ¹	R ²	hmGlu ₅ PAM EC ₅₀ ^a (nM) ¹⁹	hmGlu ₅ PAM pEC ₅₀ ^{a19}	Glu Max ^a (%) ¹⁹	HLM ^b (%)	RLM ^b (%)	clogP ^c
1	--	--	--	176	6.75 (86.73-6.78)	73 (70-76)	--	--	--
2	--	--	--	199	6.70 (6.66-6.74)	66 (63-70)	--	--	--
15b	CH ₂ -O		H	1748	5.76 (5.43-6.08)	76 (55-97)	n.t. ^d	n.t. ^d	1.7
15c	CH ₂ -O		H	1133	5.95 (5.76-6.13)	67 (55-79)	7	25	3.6
16a	O-CH ₂		H	1195	5.92 (5.84-6.01)	89 (79-99)	22	68	1.3
16b	O-CH ₂		H	696	6.16 (5.99-6.32)	76 (67-85)	72	99	1.8
16c	O-CH ₂		H	1211	5.92 (5.60-6.24)	42 (28-55)	n.t. ^d	n.t. ^d	2.1
16d	O-CH ₂		H	2314	5.64 (5.43-5.85)	66 (49-83)	n.t. ^d	n.t. ^d	1.6
16e	O-CH ₂		H	1459	5.84 (5.61-6.06)	66 (54-79)	n.t. ^d	n.t. ^d	1.8
16f	O-CH ₂		H	250	6.60 (6.34-6.86)	73 (55-91)	46	99	2.3
16g	O-CH ₂		H	851	6.07 (5.86-6.28)	71 (60-81)	n.t. ^d	n.t. ^d	1.5
16h	O-CH ₂		H	96	7.02 (6.78-7.25)	79 (63-95)	3	44	3.2
16i	O-CH ₂		H	66	7.18 (6.95-7.41)	69 (54-83)	14	43	3.2
16j	O-CH ₂		2-F	553	6.26 (6.09-6.43)	72 (64-80)	n.t. ^d	n.t. ^d	3.3
16k	O-CH ₂		3-F	77	7.12 (6.85-7.38)	61 (40-83)	18	48	3.5
16l	O-CH ₂		4-F	739	6.13 (6.02-6.24)	79 (73-85)	n.t. ^d	n.t. ^d	3.5
16m	O-CH ₂		H	1019	5.99 (5.82-6.16)	78 (69-88)	13	99	1.6

Table 1. continued

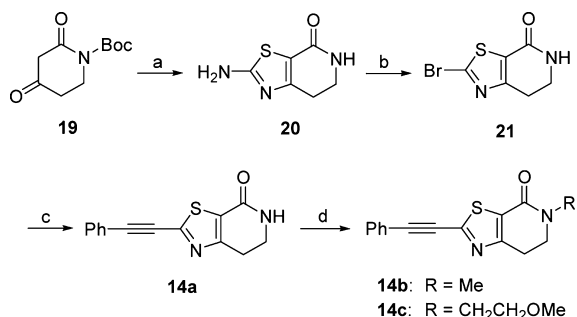
Comp	X-Y	R ¹	R ²	hmGlu ₅ PAM EC ₅₀ ^a (nM) ¹⁹	hmGlu ₅ PAM pEC ₅₀ ^{a19}	Glu Max ^a (%) ¹⁹	HLM ^b (%)	RLM ^b (%)	clogP ^c
16n	O-CH ₂		H	1759	5.75 (5.59-5.91)	77 (64-90)	n.t. ^d	n.t. ^d	1.6
16o	O-CH ₂		H	2690 ^e	5.57 ^e	82 ^e	n.t. ^d	n.t. ^d	1.6
16p	O-CH ₂		H	621	6.21 (6.12-6.29)	94 (89-99)	9	29	1.8
16q	O-CH ₂		H	791	6.10 (5.74-6.46)	56 (41-70)	33	97	1.6

^aValues were calculated from three independent experiments using a four-parameter logistic nonlinear regression model taking into account the heterogeneity between experiments and concentration–response curves for each compound. ^bHLM and RLM data refer to % of compound metabolized after incubation of tested compound with human and rat microsomes respectively, for 15 min at 1 μ M concentration. ^cCalculated with Biobyte software. ^dNot tested. ^eData obtained from a single experiment not replicated.

Scheme 1^a

^aReagents and conditions: (a) Isoamyl nitrite, CuBr₂, CH₃CN, 80 °C, 1 h, 75%; (b) phenyl acetylene, [1,1'-bis(diphenylphosphino)ferrocene]dichloro-palladium(II), CuI, Et₃N, 1,4-dioxane, reflux, 2 h, 52%.

The synthesis of the targeted compounds **14a–c** is shown in Scheme 2. Starting from commercially available Boc-protected 2,4-dioxopiperidine **19**, bromination and condensation with thiourea in the presence of sodium hydrogen carbonate followed by Boc deprotection afforded key intermediate **20** (17% overall yield), which was transformed into the dihydrothiazolopyridone **14a** with moderate yield (55%)

Scheme 2^a

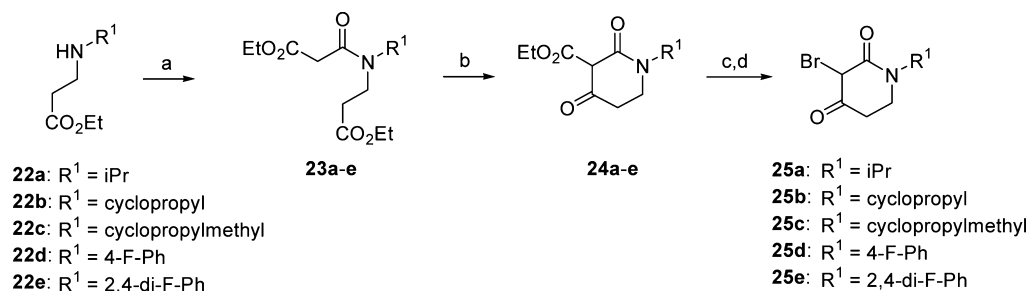
^aReagents and conditions: (a) (i) NBS, CCl₄, 10–15 °C, 2 h; (ii) thiourea, NaHCO₃, EtOH, 80 °C, 2.5 h; (iii) HCl, 1,4-dioxane, rt, 30 min, 100%; (b) isoamyl nitrite, CuBr₂, CH₃CN, rt, 1.5 h, 55%; (c) phenyl acetylene, [1,1'-bis(diphenylphosphino)ferrocene]dichloro-palladium(II), CuI, Et₃N, 1,4-dioxane, reflux, 30%; (d) **14b**, MeI or **14c**, MeOCH₂CH₂Br, Cs₂CO₃, CH₃CN, 80 °C, 16 h, 19% for **14b** and 20% for **14c**.

following an analogous procedure to the one described for the synthesis of compound **13** in Scheme 1. Finally, reaction of **14a** with the corresponding alkyl halides in the presence of cesium carbonate as base, yielded derivatives **14b,c** (19 and 20% yield, respectively).

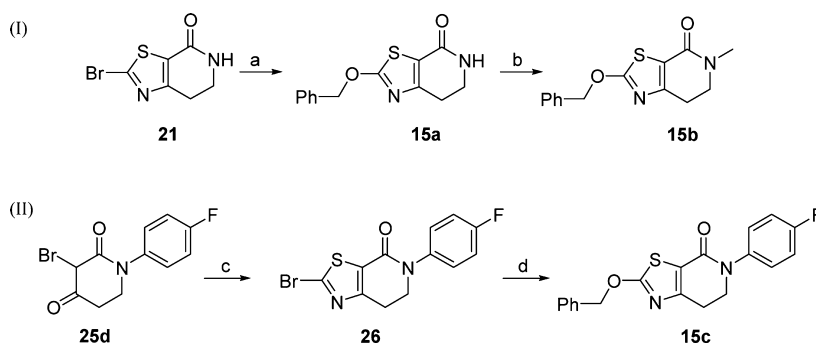
The synthetic methods used for the preparation of the final compounds **15b,c** and **16a–q** are outlined in Schemes 3–9. Preparation of most dihydrothiazolopyridones **15–16** followed a cyclization step performed with a piperidine-2,4-dione, which was commercially available or was prepared using a synthetic sequence shown in Scheme 3. Thus, commercially available β -amino esters **22a–e** were reacted with ethyl malonyl chloride to afford the amides **23a–e** in moderate to good yields (22–70%). Intramolecular cyclization reaction of **23a–e**, promoted by sodium ethoxide, yielded the corresponding 3-carbethoxypiperidine-2,4-dione derivatives **24a–e**. Acid mediated decarboxylation of **24a–e** followed by regioselective bromination afforded the key intermediates **25a–e** in good yields. These intermediates were found to be highly unstable and had to be used immediately after synthesis.

The benzyloxy-dihydrothiazolopyridones **15b,c** were prepared as shown in Scheme 4. Nucleophilic substitution of the bromothiazolopyridone **21** with benzyl alcohol yielded the target intermediate **15a**, which was subsequently *N*-alkylated with methyl iodide affording compound **15b** in 30% yield (equation (I), Scheme 4). Attempts to perform a copper catalyzed *N*-arylation reaction on **15a** (CuI, K₃PO₄, DMF, microwave irradiation) were unsuccessful as compound **15c** was found to be unstable under these reaction conditions, and the synthesis of compound **15c** was carried out as shown in the equation (II) of Scheme 4. Thus, intermolecular cyclization of **25d** with thiourea followed by Sandmeyer reaction led with low yield to the intermediate *N*-aryl bromothiazole derivative **26**, which was treated with benzyl alcohol in the presence of sodium hydride to yield (63%) the target compound **15c**.

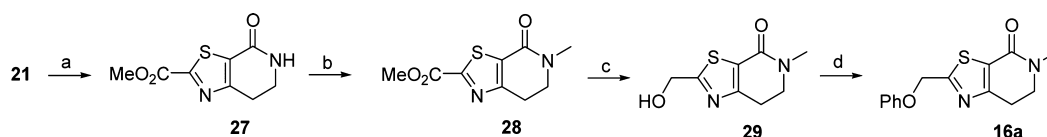
In the case of the phenoxymethyl-dihydrothiazolopyridones **16**, five main synthesis routes (Schemes 5–9) were used to access the final compounds **16a–q**. Starting from the bromothiazole derivative **21**, palladium catalyzed carbonylation

Scheme 3^a

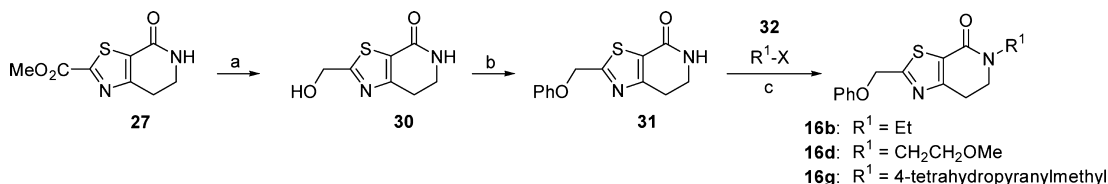
^aReagents and conditions: (a) Ethyl malonyl chloride, Et₃N or DIPEA, CH₂Cl₂, rt, 1 h, 22–70%; (b) NaOEt, EtOH, 85 °C, 16 h, 55–91%; (c) **24a–c**, CH₃CO₂H, H₂O, 90 °C, 16 h, 53–73%; or **24d,e**, CH₃CN, H₂O, 90 °C, 2 h; (d) NBS, CH₂Cl₂, 0 °C, 30 min, 73–76%.

Scheme 4^a

^aReagents and conditions: (a) BnOH, NaH, THF, 120 °C, 15 min, microwave, 54%; (b) MeI, NaH, THF, 120 °C, 15 min, microwave, 54%; (c) (i) thiourea, NaHCO₃, EtOH, 80 °C, 1 h; (ii) isoamyl nitrite, CuBr₂, CH₃CN, rt, 45 min, 16%; (d) BnOH, NaH, THF, 120 °C, 15 min, microwave, 63%.

Scheme 5^a

^aReagents and conditions: (a) CO, [1,1'-bis(diphenylphosphino)ferrocene]dichloro-palladium(II), MeOH, Et₃N, 50 °C, 16 h, 21%; (b) MeI, Cs₂CO₃, DMF, rt, 60 h, 42%; (c) NaBH₄, MeOH, 0 °C, 30 min, 99%; (d) PhOH, di-*tert*-butyl azodicarboxylate, PPh₃, THF, 120 °C, 20 min, microwave, 20%.

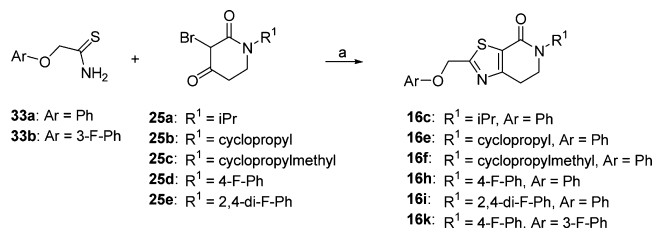
Scheme 6^a

^aReagents and conditions: (a) NaBH₄, MeOH, 0 °C, 30 min, 40%; (b) PhOH, di-*tert*-butyl azodicarboxylate, PPh₃, THF, 120 °C, 20 min, microwave, 64%; (c) **32**, Cs₂CO₃, DMF, rt, 16 h, 13–49%.

followed by alkylation with methyl iodide and reduction of the intermediate ester **28** led to the alcohol **29** which after Mitsunobu reaction with phenol afforded **16a** (Scheme 5).

Key intermediate **31** was obtained in 26% yield from intermediate **27**, in a similar way (Scheme 6). *N*-Alkylation of **31** with several primary alkyl halides **32** afforded the corresponding *N*-alkyl derivatives **16b,d,g** in moderate yields (13–49%) (Scheme 6).

Alternatively, several compounds (**16c,e,f,h,i,k**) were prepared by intermolecular cyclization between the thioamides **33a,b** and the corresponding 3-bromopiperidine-2,4-dione **25a–e** (10–25%) (Scheme 7). Similarly, derivatives **16j,l** were accessed by nucleophilic substitution on the chloromethyl thiazol **36**, obtained via reaction of **25d** with ethyl thiooxamate followed by ester reduction and subsequent treatment with thionyl chloride, with the corresponding phenols as shown in Scheme 8.

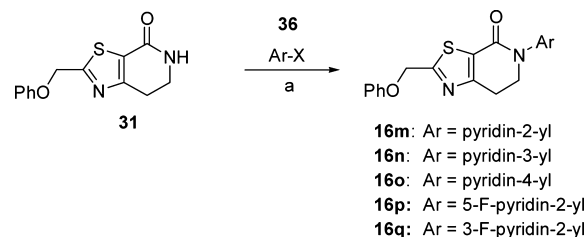
Scheme 7^a

^aReagents and conditions: (a) **25a–c**, NaHCO₃, EtOH, 70 °C, 15 min, 10–25% or **25d,e**, NaHCO₃, DMF, 100 °C, 30 min, 10–23%.

Finally, intermediate **31** was also used to prepare the *N*-pyridyl derivatives **16m–q** by copper catalyzed coupling with the corresponding halopyridines **36** as shown in Scheme 9, in low to moderate yields (15–64%).

DISCUSSION

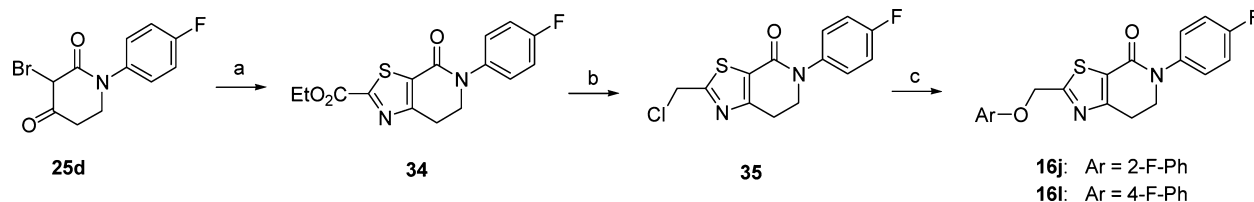
In the case of benzyloxy-dihydrothiazolopyridone derivatives **15**, our SAR investigation started with the synthesis of the methyl and 4-fluorophenyl substituted analogues **15b** (prepared by analogy to **14b**) and **15c** (selected because fluorine containing aromatic rings are common motifs as distal aromatic moieties for different mGlu₅ PAM chemotypes).^{9,16} As seen in Table 1, the introduction of the 4-fluorophenyl and the methyl substituents resulted in compounds of similar potency. Furthermore, **15c** showed good metabolic stability in human and rat fortified microsomes. Unfortunately, in the course of the aqueous solubility assessment of derivatives **15**, these were found to be unstable in acidic media (20% HP-β-CD in water, pH = 4) leading to the corresponding 2-hydroxy-dihydrothiazolopyridone fragments. In light of this finding, we decided to stop the exploration of the benzyloxy-dihydrothiazolopyridone series **15**. Instead we focused efforts on the phenoxymethyl subseries **16**, which proved to be stable under the same acidic aqueous solubility conditions. As a first step, the alkyl substituent on the amide moiety was explored. Akin to the benzyloxy series, introduction of a methyl group in **16a** resulted in a significant reduction (~6 fold) in mGlu₅ PAM potency compared to the corresponding acetylene analogue **14b**, or reference compounds **1** and **2**, but still retained high efficacy. Replacement of the methyl group in **16a** by other alkyl chains with increased size and diverse polarity either had a limited effect or was detrimental to activity. Thus, comparable activity was observed for the more lipophilic **16b** (R¹ = ethyl) and **16c** (R¹ = isopropyl), although a modest reduction in efficacy was also noted for the bulkier **16c**. In the case of the methoxyethyl substituted **16d** and in analogy with the acetylene containing series **14**, the potency was again in the same range as for **16a**.

Scheme 9^a

^aReagents and conditions: (a) **16m–o,q**, **33**, CuI, K₂CO₃, *N,N'*-dimethylethylenediamine, toluene, 120 °C, 16 h, 15–64% or **16p**, 2-bromo-4-fluoropyridine, CuI, K₃PO₄, *N,N'*-dimethylethylenediamine, toluene, 140 °C, 16 h, 64%.

The introduction of a cyclopropyl group with pseudo aromatic character in **16e** resulted as well in a similar potency when compared to **16a** and its isopropyl congener **16c**. Noteworthy, the introduction of a methylene spacer between the cyclopropyl group and the dihydrothiazolopyridone core (**16f**) delivered a remarkable increase in potency (~6 fold vs. **16a** and **16e**). Finally, ring expansion to the more polar tetrahydropyran ring (**16g**) had almost negligible effect on both potency and efficacy compared to **16a**. As observed with the benzyloxy series, better results were obtained with fluorophenyl tethered amides such as **16h** or **16i** with in vitro potencies below 100 nM (~2–3 fold more potent than reference compounds **1** and **2**) and good efficacies. Taking **16h** as a starting point, the introduction of fluorine substitution in the western aromatic ring was found to be preferred at position 3, with **16k** showing comparable potency and minimally reduced efficacy to **16h**. A ~7–10-fold decrease in potency was observed for the 2- and 4-substituted analogues **16j,l**. In light of the promising in vitro results obtained with the aryl derivatives **16h–l**, our SAR exploration concluded with the investigation of the effects of replacing the fluorophenyl amide substituents by more polar and weakly basic pyridine rings. From the data in Table 1, it can be concluded that the 2-substituted pyridine analogue **16m** was preferred over the 3 and 4 regioisomers (**16n** and **16o**). On the other hand, although 3-fluorine substitution (**16q**) did not induce any increase on mGlu₅ potency, a significant improvement was accomplished by the introduction of the fluorine atom in the 5-position of the 2-substituted pyridine ring, with **16p** showing similar potency to **16m** and increased efficacy (94% vs. 79%).

In light of their good mGlu₅ PAM activity and efficacy compounds **16a**, **16b**, **16f**, **16h**, and **16p** were selected as representative examples for further characterization. Metabolic stability evaluation showed significant species differences, with lower turnovers in human vs. rat liver microsomes in all cases.

Scheme 8^a

^aReagents and conditions: (a) Ethyl thiooxamate, NaHCO₃, EtOH, 80 °C, 2 h, 15%; (b) (i) NaBH₄, MeOH, 0 °C, 2 h; (ii) SOCl₂, CH₂Cl₂, rt, 2 h, 27%; (c) Ar-OH, K₂CO₃, DMF, rt, 24 h, 8–20%.

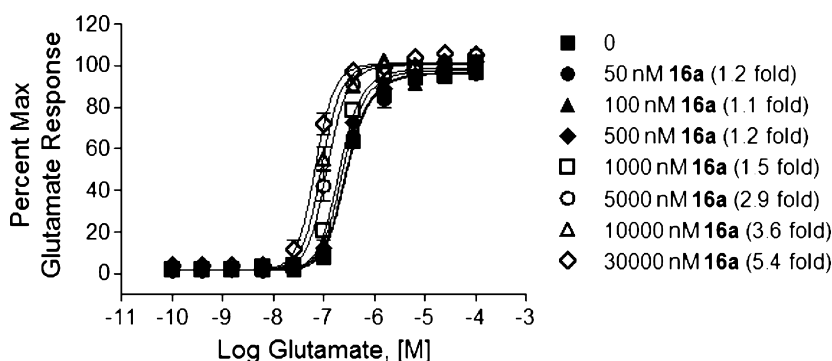


Figure 3. Glutamate CRC in the presence of increasing concentrations of **16a**.

Thus, despite low (**16a**, **16h**, and **16p**, > 75% remaining) to moderate-high (**16b** and **16f**, 75–25% remaining) turnover in HLM for the five compounds, metabolic instability in RLM ranged from moderate (**16p**, ~30% remaining) to very high (**16b** and **16f**, ~100% metabolized). As high metabolic instability in rodents would hamper further pharmacological evaluation, only compounds **16a**, **16h**, and **16p** were selected for additional DMPK evaluation to confirm their potential utility for proof-of-concept in vivo studies for this series. Thus, **16a** and **16b** were evaluated in noncrossover in vivo pharmacokinetic (PK) studies in rats. Because of its poor solubility in aqueous buffer (<4 μM , pH 7.4) and in 20% HP- β -CD in water formulation (<0.20 mg/mL), **16h** could only be dosed orally as a suspension (5 mg/mL) and was found to be undetectable in the brain after 2.0 h of administration and hence discarded for in vivo pharmacological evaluation. As a consequence of these findings, and because the improvement in kinetic solubility for **16p** was minimal (10 μM , pH 7.4 and <1 mg/mL in 20% HP- β -CD in water) compared to **16h**, **16p** was discarded for further investigation. PK studies (1 mg/kg iv, 10 mg/kg p.o.) with the more soluble **16a** (97 μM , aqueous buffer pH 7.4 and 4 mg/mL in 20% HP- β -CD in water), revealed a relatively high CL_p of 50 mL/min/kg and a short half-life ($T_{1/2}$) of 0.18 h. Examination of drug concentrations in portal vein, plasma, and brain at different time points (0.5, 1.0, 2.0, 4.0, and 7.0 h) showed a moderate first-pass clearance (E_{hep} 0.47) with a relatively low volume of distribution (V_{ss} = 0.70 L/kg) and moderate systemic exposure (plasma $_{\text{AUC}}$ = 2.9 $\mu\text{M}\cdot\text{h}$). The relative CNS exposure of **16a** was moderate as well (brain $_{\text{AUC}}$ = 2.4 $\mu\text{M}\cdot\text{h}$) with a good distribution to the brain (brain $_{\text{AUC}}$ /plasma $_{\text{AUC}}$ = 0.90). Additionally, a relatively high unbound fraction in brain (rat f_u brain = 18%) contributed favorably to achieve good absolute brain levels (C_{max} = 522 nM, T_{max} = 0.5 h), which were considered adequate to warrant further pharmacological evaluation.

Subsequent in vitro examination of **16a** in a low expressing rat receptor mGlu $_5$ cell line²⁷ resulted in a slightly reduced potency (~2 fold) and efficacy (EC_{50} = 3408 nM, 62% Glu Max) compared with the human receptor expressing cell line. **16a** was found to be selective in an mGlu selectivity panel (mGlu $_{1-4,6-8}$ EC_{50} > 10 μM)²⁰ and also when tested at 10 μM concentration in a panel of 66 off-target class receptors, ion channels and transporters.²⁸ Finally, positive allosteric modulator activity was further investigated by fold-shift experiments to determine the degree of cooperativity with glutamate of the compound. Thus, as shown in Figure 4, progressive fold-shift experiments in our cell line expressing the rat mGlu $_5$ receptor revealed how the concentration response curve of (CRC)

glutamate shifted to the left with increasing concentration of **16a** (55 nM to 30 μM) with no significant effect change of the maximal response. A 5.4-fold leftward shift in the glutamate EC_{50} was observed in the presence of 30 μM **16a**, and a predicted allosteric modulator affinity of approximately 10 μM (10069 nM) was calculated using the operational model of allosterism described by Gregory et al. (Figure 3).²⁹ These results corroborate a positive allosteric interaction between glutamate and **16a** and were confirmed in a cell line expressing the human mGlu $_5$ receptor,²⁷ where 10 μM **16a** produced a 4.4-fold leftward shift in the glutamate CRC.

Encouraged by its overall profile, **16a** (Figure 4) was evaluated in a screen of potential antipsychotic efficacy, the reversal of amphetamine-induced hyperlocomotion in rats.^{10,11}

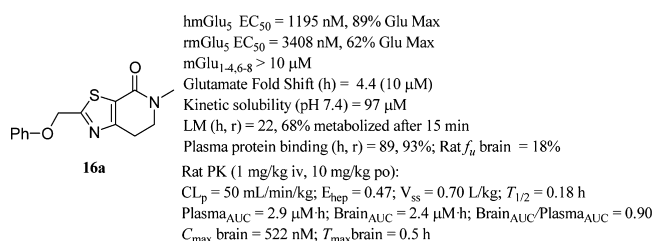


Figure 4. Profile summary of **16a**.

As seen in Figure 5, when dosed orally in a 20% HP- β -CD in water formulation, **16a** showed robust dose-dependent effects in reversal of hyperlocomotion with a lowest active oral dose of 10 mg/kg. The maximal effect (61%) was seen at the highest tested dose of 100 mg/kg, corresponding with an estimated average terminal unbound brain concentration of ~3.2 μM ,³⁰ which is well in line with the rat in vitro mGlu $_5$ PAM EC_{50} of **16a** and that, according with the progressive fold-shift experiments (Figure 3), would correlate with a left-ward shift in the glutamate CRC in the range of ~1.5–2.9 fold.

The preliminary in vivo characterization of **16a** concluded with the evaluation of balance and motor coordination and potential neurological side effects by means of rotarod and Irwin modified neurological battery tests respectively in rats. As it can be seen in Figure 6, when dosed orally at 30, 56.6, and 100 mg/kg (20% HP- β -CD in water), **16a** had no statistically significant effect on general motor output as measured by performance on the rotarod (120 s cutoff) test in rats.³¹ Furthermore, **16a** had no effect on any autonomic or somatomotor nervous system functions as measured using the modified Irwin neurological test battery in rats when tested at a single oral dose of 100 mg/kg (20% HP- β -CD in water).³²

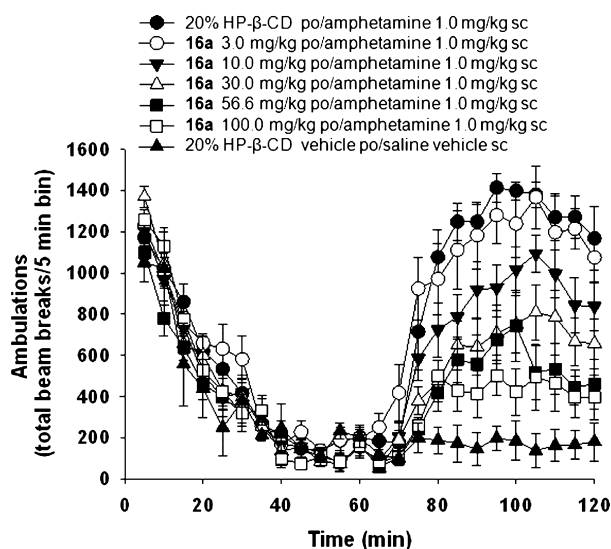


Figure 5. Dose-dependent effect of **16a** on the reversal of amphetamine-induced hyperlocomotion in rats.

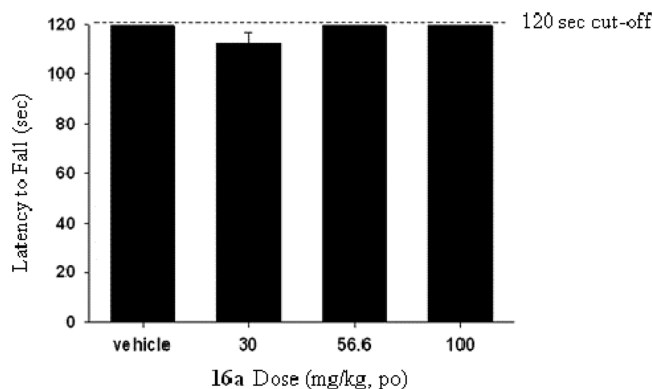


Figure 6. Effects of **16a** on rotarod performance in rats.

These results highlight how **16a** neither impacts motor behavior nor shows any overt neurological side effects in rats up to a dose of 100 mg/kg p.o., a dose that has been previously shown to produce maximal efficacy in the inhibition of the amphetamine-induced hyperlocomotion.

CONCLUSIONS

In summary, starting from a singleton phenyl ester chromanone HTS hit, two parallel approaches allowed the identification of the benzyloxy and phenoxyethyl moieties and the dihydrothiazolopyridone core as optimal replacements for the ester and the chromanone core respectively. While the benzyloxy-dihydrothiazolopyridone subseries was found susceptible to hydrolysis, the phenoxyethyl-dihydrothiazolopyridones **16** proved to be a promising mGlu₅ PAM series. Preliminary focused SAR exploration of amide substituents revealed aromatic groups as preferred substituents for achieving high in vitro mGlu₅ potentiation although their poor DMPK characteristics precluded further in vivo evaluation. On the other hand, the *N*-methyl analogue **16a** presented a more balanced profile in terms of in vitro potency, selectivity and DMPK profile, which made it an attractive candidate for in vivo characterization in a model of antipsychotic activity. **16a** showed robust, dose-dependent effects in the reversal of amphetamine induced hyperlocomotion, with a lowest active

dose of 10 mg/kg p.o. and maximal efficacy at a dose of 100 mg/kg p.o. without showing any significant motor impairment or overt neurological side effects up to a dose of 100 mg/kg p.o. These results underscore the potential of **16a** as an interesting tool compound suitable to unravel the in vivo pharmacology of mGlu₅ positive allosteric modulation. Further investigation and evolution of this novel series of mGlu₅ PAMs are underway and will be reported in due course.

EXPERIMENTAL SECTION

Chemistry. Unless otherwise noted, all reagents and solvents were obtained from commercial suppliers and used without further purification. Thin layer chromatography (TLC) was carried out on silica gel 60 F254 plates (Merck). Flash column chromatography was performed on silica gel, particle size 60 Å, mesh of 230–400 (Merck) under standard techniques. Microwave assisted reactions were performed in a single-mode reactor, Biotage Initiator Sixty microwave reactor (Biotage), or in a multimode reactor, MicroSYNTH Labstation (Milestone, Inc.). Nuclear magnetic resonance (NMR) spectra were recorded with a Bruker DPX-300 or a Bruker DPX-400 or a Bruker AV-500 spectrometer (Bruker AG) with standard pulse sequences, operating at 300, 400, and 500 MHz, respectively, using CDCl₃ and DMSO-*d*₆ as solvents. Chemical shifts (δ) are reported in parts per million (ppm) downfield from tetramethylsilane (δ = 0). Coupling constants are reported in Hertz. Splitting patterns are defined by s (singlet), d (doublet), dd (double doublet), t (triplet), q (quartet), quin (quintet), sex (sextet), sep (septet), or m (multiplet). Liquid chromatography combined with mass spectrometry (LCMS) was performed on either a HP 1100 high-performance liquid chromatography (HPLC) system (Agilent Technologies) or Advanced Chromatography Technologies system composed of a quaternary or binary pump with degasser, an autosampler, a column oven, a diode array detector (DAD), and a column as specified in the respective methods below. Flow from the column was split to a MS spectrometer. The MS detector was configured with either an electrospray ionization source or an electrospray combined with atmospheric pressure chemical ionization (ESCI) dual ionization source. Nitrogen was used as the nebulizer gas. Data acquisition was performed with MassLynx-Openlynx software or with Chemstation-Agilent data browser software. More detailed information about the different LCMS methods employed can be found in the Supporting Information. Liquid chromatography combined with high resolution mass spectrometry (LC-HRMS) was performed using a Micromass (Waters) Q-ToF API-US calibrated and verified with sodium iodide. The samples were diluted with a 50:50 0.1% formic acid (in Milli-Q)/acetonitrile solution, directly infused using leucine-enkephalin ($[M + H]^+$ = 556.2771) as a lockmass. Scan range was from 100 to 1000 Da, with a scan time of 1 s. For a number of compounds, melting points (M_p^a) were determined with a WRS-2A melting point apparatus (Shanghai Precision and Scientific Instrument Co. Ltd.). Melting points were measured with a linear heating up rate of 0.2–5.0 °C/min (maximum temperature 300 °C), and the reported values are melt ranges. For another number of compounds, melting points (M_p^b) were determined in open capillary tubes on a FP62 or on a FP81HT-FP90 apparatus (Mettler). Melting points were measured with a temperature gradient of 10 °C/min (maximum temperature 300 °C), and the melting point was read from a digital display. Melting point values are peak values and were obtained with experimental uncertainties that are commonly associated with this analytical method.

Purities of all new compounds were determined by analytical reversed-phase high-performance liquid chromatography (RP-HPLC) using the area percentage method on the UV trace recorded at a wavelength of 254 nm, and compounds were found to have $\geq 95\%$ purity unless otherwise specified.

2-Bromo-5,6-dihydro-4H-benzothiazol-7-one (18). A mixture of **17**²⁷ (19 g, 112 mmol), CuBr₂ (27 g, 120 mmol), and 3-methyl-1-nitrosooxy-butane (18 g, 153 mmol) in CH₃CN (250 mL) was stirred at 80 °C for 1 h. The mixture was then cooled to rt and poured into a

10% solution of HCl. The mixture was extracted with CH_2Cl_2 and the organic layer was separated, dried (Na_2SO_4), and filtered, and the solvent was evaporated in vacuo to yield 19.6 g (75%) of **18** that was used in the next step without any further purification. ^1H NMR (500 MHz, CDCl_3) δ ppm 2.47–2.60 (m, 2 H), 3.07–3.15 (m, 1 H), 3.18–3.29 (m, 1 H), 4.64 (t, J = 3.9 Hz, 1 H).

2-Amino-6,7-dihydro-5H-thiazolo[5,4-c]pyridin-4-one hydrochloride salt (20). To a solution of **19** (40 g, 187.58 mmol) in CCl_4 (500 mL) was added NBS (33.38 g, 187.58 mmol) portionwise keeping the reaction temperature in the range of 10–15 °C. The mixture was further stirred at 10–15 °C for 2 h. The mixture was allowed to warm to rt, and the solvent was evaporated in vacuo. The residue thus obtained was dissolved in EtOAc and washed with H_2O . The organic layer was separated, dried (Na_2SO_4), and filtered and the solvent was evaporated. The residue thus obtained was dissolved in EtOH (400 mL), and then thiourea (6.5 g, 85.6 mmol) and NaHCO_3 (7.2 g, 85.6 mmol) were added. The resulting mixture was stirred at 80 °C for 2.5 h and then cooled to rt, and the solids were filtered off. The filtrate was evaporated in vacuo to give a residue that was crystallized in EtOH. The yellow crystals thus obtained were dissolved in a 4 M solution of HCl in 1,4-dioxane (100 mL), and the resulting mixture was stirred at rt for 30 min. The solvent was evaporated in vacuo to yield 10 g (88% pure) of **20** as a yellow powder which was used in the next step without any further purification. LCMS: m/z 170 $[\text{M} + \text{H}]^+$, t_R = 0.38 min.

2-Bromo-6,7-dihydro-5H-thiazolo[5,4-c]pyridin-4-one (21). A mixture of **20** (8 g, 39.8 mmol), CuBr_2 (10.43 g, 46.68 mmol), and 3-methyl-1-nitrosooxy-butane (6.8 g, 58.35 mmol) in CH_3CN (100 mL) was stirred at rt for 1.5 h. The solvent was evaporated in vacuo. The residue thus obtained was dissolved in EtOAc and washed with H_2O . The organic layer was separated, dried (Na_2SO_4), and filtered, and the solvent was evaporated in vacuo to yield 5 g (55%) of **21** that was used in the next step without any further purification. LCMS: m/z 233 $[\text{M} + \text{H}]^+$, t_R = 0.70 min.

N-(2-Ethoxycarbonyl-ethyl)-N-isopropyl-malonamic Acid Ethyl Ester (23a). To a solution of **22a** (13.5 g, 69 mmol) in CH_2Cl_2 (100 mL) was added Et_3N (26 g, 255 mmol). Then ethyl malonyl chloride (14 g, 93 mmol) was added to the mixture at 0 °C, and the mixture was stirred at rt for 5 h. Then H_2O was added and the organic layer was separated, dried (Na_2SO_4), and filtered and the solvent was evaporated in vacuo. The crude product was purified by flash column chromatography (silica gel, EtOAc in petroleum ether, 10/90 to 33/66). The desired fractions were collected and the solvents evaporated in vacuo to yield 5.1 g (87% pure) of **23a** as an oil. LCMS: m/z 274 $[\text{M} + \text{H}]^+$, t_R = 1.25 min.

N-Cyclopropyl-N-(2-ethoxycarbonyl-ethyl)-malonamic Acid Ethyl Ester (23b). Starting from **22b** (40.3 g, 256 mmol) and following the procedure described for **23a**, **23b** was obtained as an oil (40 g, 60% pure). LCMS: m/z 272 $[\text{M} + \text{H}]^+$, t_R = 0.91 min.

N-Cyclopropylmethyl-N-(2-ethoxycarbonyl-ethyl)-malonamic Acid Ethyl Ester (23c). Starting from **22c** (31.3 g, 183 mmol) and following the procedure described for **23a**, **23c** was obtained as an oil (33 g, 93% pure). LCMS: m/z 286 $[\text{M} + \text{H}]^+$, t_R = 1.23 min.

N-(2-Ethoxycarbonyl-ethyl)-N-(4-fluoro-phenyl)-malonamic Acid Ethyl Ester (23d). Starting from **22d** (10 g, 47.3 mmol) and following the procedure described for **23a** but using diisopropylethylamine as base, **23d** was obtained as an orange oil (11 g, 73% pure). LCMS: m/z 326 $[\text{M} + \text{H}]^+$, t_R = 2.41 min.

N-(2-Ethoxycarbonyl-ethyl)-N-(2,4-difluoro-phenyl)-malonamic Acid Ethyl Ester (23e). Starting from **22e** (29 g, 127 mmol) and following the procedure described for **23a**, **23e** was obtained as an orange oil (35 g, 69% pure). LCMS: m/z 344 $[\text{M} + \text{H}]^+$, t_R = 1.21 min.

1-Isopropyl-2,4-dioxo-piperidine-3-carboxylic Acid Ethyl Ester (24a). Sodium (0.86 g, 37.3 mmol) was added to EtOH (50 mL) at 0 °C. The mixture was stirred at rt for 1 h. Then **23a** (5.1 g, 18.6 mmol) was added and the mixture was stirred at 85 °C for 16 h. The mixture was poured into ice H_2O . The aqueous phase was neutralized by addition of a 2 N HCl solution and extracted with EtOAc. The organic layer was separated, dried (Na_2SO_4), and filtered, and the solvent was evaporated in vacuo to yield 3 g (91%) of **24a** which was

used in the next step without any further purification. LCMS: m/z 228 $[\text{M} + \text{H}]^+$, t_R = 0.95 min.

1-Cyclopropyl-2,4-dioxo-piperidine-3-carboxylic Acid Ethyl Ester (24b). Starting from **23b** (40 g, 147 mmol) and following the procedure described for **24a**, **24b** was obtained as an oil (20 g, 61%). LCMS: m/z 226 $[\text{M} + \text{H}]^+$, t_R = 0.91 min.

1-Cyclopropylmethyl-2,4-dioxo-piperidine-3-carboxylic Acid Ethyl Ester (24c). Starting from **23c** (20 g, 70.1 mmol) and following the procedure described for **24a**, **24c** was obtained as an oil (10 g, 60%). LCMS: m/z 240 $[\text{M} + \text{H}]^+$, t_R = 1.21 min.

1-(4-Fluoro-phenyl)-2,4-dioxo-piperidine-3-carboxylic Acid Ethyl Ester (24d). A mixture of **23d** (6.27 g, 19.27 mmol) in a 21% solution of sodium ethoxide in EtOH (14.39 mL, 38.55 mmol) was stirred at 85 °C for 16 h. The solvent was evaporated in vacuo and the residue was partitioned between EtOAc and H_2O . The aqueous layer was separated, acidified by 1N HCl solution addition and extracted with CH_2Cl_2 . The organic layer was separated, dried (Na_2SO_4), filtered and the solvent evaporated in vacuo to yield 5 g (66% pure) of **24d** which was used in the next step without any further purification. LCMS: m/z 280 $[\text{M} + \text{H}]^+$, t_R = 0.73 min.

1-(2,4-Difluoro-phenyl)-2,4-dioxo-piperidine-3-carboxylic acid ethyl ester (24e). Starting from **23e** (4.8 g, 13.98 mmol) and following the procedure described for **24d**, **24e** was obtained as an oil (4.16 g, 55% pure). LCMS: m/z 298 $[\text{M} + \text{H}]^+$, t_R = 0.65 min.

3-Bromo-1-isopropyl-piperidine-2,4-dione (25a). A solution of **24a** (3 g, 13.2 mmol) in a mixture of acetic acid (10 mL) and H_2O (90 mL) was stirred at 90 °C for 14 h. The mixture was cooled and extracted with CH_2Cl_2 . The organic layer was separated, dried (Na_2SO_4), and filtered, and the solvent was evaporated in vacuo. The crude product was purified by flash column chromatography (silica gel; EtOAc in petroleum ether 10/90 to 33/66). The desired fractions were collected and the solvents evaporated in vacuo. The residue thus obtained was dissolved in CH_2Cl_2 (20 mL) and NBS (1.1 g, 6.44 mmol) was added. The mixture was stirred at rt for 4 h. Then H_2O was added and the mixture was extracted with EtOAc. The organic layer was separated, dried (Na_2SO_4), and filtered, and the solvents were evaporated in vacuo to yield 0.6 g (53% pure) of **26a** which was used in the next step without any further purification. LCMS: m/z 234 $[\text{M} + \text{H}]^+$, t_R = 0.35 min.

3-Bromo-1-cyclopropyl-piperidine-2,4-dione (25b). Starting from **24b** (20 g, 89 mmol) and following the procedure described for **25a**, **25b** was obtained as an oil (11 g, 73% pure). LCMS: m/z 232 $[\text{M} + \text{H}]^+$, t_R = 0.29 min.

3-Bromo-1-cyclopropylmethyl-piperidine-2,4-dione (25c). Starting from **24c** (10 g, 41.8 mmol) and following the procedure described for **25a**, **25c** was obtained as an oil (4 g, 66% pure). LCMS: m/z 246 $[\text{M} + \text{H}]^+$, t_R = 1.053 min.

3-Bromo-1-(4-fluoro-phenyl)-piperidine-2,4-dione (25d). Starting from **24d** (7.5 g, 26.86 mmol) and following the procedure described for **25a**, **25d** was obtained as an oil (7.7 g, 76% pure). LCMS: m/z 285 $[\text{M} + \text{H}]^+$, t_R = 0.42 min.

3-Bromo-1-(2,4-difluoro-phenyl)-piperidine-2,4-dione (25e). Starting from **24e** (18 g, 60 mmol) and following the procedure described for **25a**, **25e** was obtained as an oil (11 g, 38% pure). LCMS: m/z 304 $[\text{M} + \text{H}]^+$, t_R = 0.34 min.

2-Bromo-5-(4-fluoro-phenyl)-6,7-dihydro-5H-thiazolo[5,4-c]pyridin-4-one (26). A mixture of **25d** (4.14 g, 14.48 mmol), thiourea (1.1 g, 14.48 mmol) and NaHCO_3 (1.22 g, 14.48 mmol) in EtOH (60 mL) was stirred at 80 °C for 1 h. The mixture was then cooled to rt and the solids were filtered off. The filtrate was evaporated in vacuo. The residue thus obtained was dissolved in CH_3CN (80 mL) and then CuBr_2 (3.05 g, 13.67 mmol) and 3-methyl-1-nitrosooxy-butane (2.3 mL, 17.09 mmol) were added. The mixture was stirred at rt for 45 min and then the solvent was evaporated in vacuo. The residue thus obtained was partitioned between EtOAc and H_2O . The organic layer was separated, dried (Na_2SO_4), filtered and the solvent evaporated in vacuo. The crude product was purified by flash column chromatography (silica gel, EtOAc in heptane, 0/100 to 30/70). The desired fractions were collected and the solvents evaporated in vacuo to yield

1.2 g (16%) of **26** as a white solid. LCMS: m/z 327 $[M + H]^+$, $t_R = 2.51$ min.

4-Oxo-4,5,6,7-tetrahydro-thiazolo[5,4-*c*]pyridine-2-carboxylic acid methyl ester (27). A mixture of Et_3N (17.2 g, 171 mmol) and $[1,1'$ -bis(diphenylphosphino)ferrocene]dichloro-palladium(II) (2 g, 2.7 mmol) in THF (300 mL) was added to a solution of **21** (7.5 g, 23.6 mmol) in MeOH (300 mL). Then the mixture was stirred at 50 °C overnight under CO atmosphere (2.5 MPa). The mixture was cooled and filtered, and the solvents were evaporated in vacuo. The crude product was purified by flash column chromatography (silica gel, MeOH in CH_2Cl_2 , 1/99). The desired fractions were collected and evaporated in vacuo to yield 4.5 g (21%) of **27** that crystallized from EtOAc as a yellow solid. Mp^a 217.6–220.0 °C. 1H NMR (300 MHz, $CDCl_3$) δ ppm 3.20 (t, $J = 7.1$ Hz, 2 H), 3.62–3.79 (m, 2 H), 4.02 (s, 3 H), 5.84 (br. s., 1 H). LCMS: m/z 213 $[M + H]^+$, $t_R = 2.94$ min.

5-Methyl-4-oxo-4,5,6,7-tetrahydro-thiazolo[5,4-*c*]pyridine-2-carboxylic acid methyl ester (28). Iodomethane (4.4 mL, 70.7 mmol) was added to a suspension of **27** (10 g, 47.1 mmol) and Cs_2CO_3 (23 g, 70.68 mmol) in DMF (118 mL) under nitrogen. The mixture was stirred at rt for 60 h and then diluted with H_2O and extracted with EtOAc. The organic layer was separated, dried ($MgSO_4$), and filtered, and the solvent was evaporated in vacuo. The crude product was purified by flash column chromatography (silica gel, EtOAc in CH_2Cl_2 , 0/100 to 50/50). The desired fractions were collected, and the solvents were evaporated in vacuo to yield 4.46 g (42%) of **28** as a pale brown oily solid. 1H NMR (400 MHz, $CDCl_3$) δ ppm 3.13 (s, 3 H), 3.23 (t, $J = 7.2$ Hz, 2 H), 3.71 (t, $J = 7.2$ Hz, 2 H), 4.03 (s, 3 H). LCMS: m/z 227 $[M + H]^+$, $t_R = 0.60$ min.

2-Hydroxymethyl-5-methyl-6,7-dihydro-5H-thiazolo[5,4-*c*]pyridin-4-one (29). Sodium borohydride (0.15 g, 4.0 mmol) was added to a stirred solution of **28** (0.65 g, 2.87 mmol) in a mixture of THF (8.8 mL) and MeOH (8.8 mL). The mixture was stirred at 0 °C for 30 min in a sealed tube under nitrogen and then diluted with H_2O and extracted with CH_2Cl_2 . The organic layer was separated, dried (Na_2SO_4), and filtered and the solvents were evaporated in vacuo. The aqueous phase was acidified with 3 N HCl and extracted with CH_2Cl_2 . The combined organic layers were dried (Na_2SO_4) and filtered, and the solvents were evaporated in vacuo. The crude product was purified by flash column chromatography (silica gel, MeOH in EtOAc, 0/100 to 20/80). The desired fractions were collected and the solvents were evaporated in vacuo to yield 0.59 g (99%) of **29** as a dark oil. 1H NMR (400 MHz, $CDCl_3$) δ ppm 2.81 (t, $J = 6.1$ Hz, 1H), 3.10 (t, $J = 7.2$ Hz, 2 H), 3.10 (s, 3 H), 3.66 (t, $J = 7.2$ Hz, 2 H), 4.93 (d, $J = 6.2$ Hz, 2 H). LCMS: m/z 199 $[M + H]^+$, $t_R = 0.28$ min.

2-Hydroxymethyl-6,7-dihydro-5H-thiazolo[5,4-*c*]pyridin-4-one (30). Starting from **27** (10 g, 47 mmol) and following the procedure described for **29**, **30** was obtained as an oil (3.5 g, 40%). Mp^a 212.1–230.9 °C. 1H NMR (400 MHz, DMSO- d_6) δ ppm 2.92 (t, $J = 7.0$ Hz, 2 H), 3.47 (td, $J = 7.0, 2.5$ Hz, 2 H), 4.72 (s, 2 H), 6.24 (br. s., 1 H), 7.79 (br. s., 1 H). LCMS: m/z 185 $[M + H]^+$, $t_R = 3.63$ min.

2-Phenoxy-methyl-6,7-dihydro-5H-thiazolo[5,4-*c*]pyridin-4-one (31). Di-*tert*-butyl azodicarboxylate (3.0 g, 13.03 mmol) was added to a stirred solution of **30** (2 g, 10.86 mmol), phenol (1.23 g, 13.03 mmol), and PPh_3 (3.42 g, 13.03 mmol) in THF (31 mL) under nitrogen. The mixture was stirred at 120 °C for 40 min under microwave irradiation. The solvent was evaporated in vacuo. The crude product was purified by flash column chromatography (silica gel, EtOAc in CH_2Cl_2 , 0/100 to 100/0). The desired fractions were collected and evaporated in vacuo to yield 1.82 g (69% pure) of **31** as a white solid. LCMS: m/z 261 $[M + H]^+$, $t_R = 1.50$ min.

2-Phenoxy-thioacetamide (33a). To a solution of phenoxyacetonitrile (38 g, 285 mmol) in DMF (380 mL), thioacetamide (42.8 g, 450 mmol) and a solution of 4 M HCl in 1,4-dioxane (380 mL) were added. The mixture was stirred at 100 °C for 16 h and then cooled to rt and poured into a saturated solution of $NaHCO_3$. The solid formed was filtered off, washed with H_2O , and dried in vacuo to yield 45 g (94%) of **33a** as a beige solid which was used in the next step without any further purification. 1H NMR (500 MHz, $CDCl_3$) δ ppm 4.88 (s, 2 H), 6.89–6.97 (m, 2 H), 7.04 (t, $J = 7.4$ Hz, 1 H), 7.29–7.36 (m, 2

H), 7.74 (br. s, 1 H), 7.97 (br. s, 1 H). LCMS: m/z 166 $[M - H]^-$, $t_R = 1.18$ min.

2-(3-Fluoro-phenoxy)-thioacetamide (33b). Starting from (3-fluoro-phenoxy)-acetonitrile (3.39 g, 22.41 mmol) and thioacetamide (4.21 g, 56.02 mmol) and following the procedure described for **33a**, **33b** was obtained as a white solid (3.58 g, 86%). 1H NMR (400 MHz, DMSO- d_6) δ ppm 4.78 (s, 2 H), 6.70–6.91 (m, 3 H), 7.25–7.42 (m, 1 H), 9.69 (m, 2 H). LCMS: m/z 184 $[M - H]^-$, $t_R = 1.19$ min.

5-(4-Fluoro-phenyl)-4-oxo-4,5,6,7-tetrahydro-thiazolo[5,4-*c*]pyridine-2-carboxylic acid ethyl ester (34). A mixture of **25d** (11.8 g, 41.3 mmol), ethyl thiooxamate (5.5 g, 41.3 mmol), and $NaHCO_3$ (8.7 g, 103.5 mmol) in EtOH (400 mL) was stirred at 80 °C for 2 h. The mixture was cooled and filtered, and the filtrate was evaporated in vacuo. The crude product was purified by flash column chromatography (silica gel, EtOAc in petroleum ether, 10/90 to 33/66). The desired fractions were collected and evaporated in vacuo to yield 2 g (68% pure) of **34**. LCMS: m/z 321 $[M + H]^+$, $t_R = 1.05$ min.

2-Chloromethyl-5-(4-fluoro-phenyl)-6,7-dihydro-5H-thiazolo[5,4-*c*]pyridin-4-one (35). Sodium borohydride (0.7 g, 18.7 mmol) was added to a solution of **34** (2 g, 6.3 mmol) in MeOH (50 mL) at 0 °C. The mixture was stirred at rt for 2 h, H_2O was added, and the mixture was extracted with EtOAc. The organic layer was separated, dried (Na_2SO_4), and filtered, and the solvent was evaporated in vacuo. The crude product was purified by flash column chromatography (silica gel, EtOAc in petroleum ether, 20/80 to 66/33). The desired fractions were collected, and the solvents were evaporated in vacuo. The residue thus obtained was added to a mixture of thionyl chloride (10 mL) and CH_2Cl_2 (10 mL). The mixture was stirred at rt for 2 h. The solvents were then evaporated in vacuo to yield 1 g (87% pure) of **35** as a solid which was used in the next step without any further purification. LCMS: m/z 297 $[M + H]^+$, $t_R = 1.03$ min.

2-Phenylethynyl-5,6-dihydro-4H-benzothiazol-7-one (13). To a solution of **18** (2.3 g, 9.86 mmol), phenylacetylene (2.01 g, 19.7 mmol), CuI (0.2 g, 1.05 mmol) and Et_3N (2.98 g, 29.58 mmol) in 1,4-dioxane (50 mL) at rt was added $[1,1'$ -bis(diphenylphosphino)ferrocene]dichloro-palladium(II) (0.2 g, 0.25 mmol). The mixture was stirred at reflux for 2 h under nitrogen. The solvent was evaporated in vacuo. The crude product was purified by flash column chromatography (silica gel, EtOAc in petroleum ether, 66/33). The desired fractions were collected, and the solvent was evaporated in vacuo to yield 1.2 g (52%) of **13** as a solid. Mp^a 117.1–119.9 °C. 1H NMR (400 MHz, $CDCl_3$) δ ppm 2.28 (quin, $J = 6.4$ Hz, 2 H), 2.70 (t, $J = 6.3$ Hz, 2 H), 3.13 (t, $J = 6.1$ Hz, 2 H), 7.39–7.53 (m, 3 H), 7.60–7.70 (m, 2 H). LCMS: m/z 254 $[M + H]^+$, $t_R = 5.49$ min.

2-Phenylethynyl-6,7-dihydro-5H-thiazolo[5,4-*c*]pyridin-4-one (14a). To a solution of **21** (2.33 g, 10 mmol), phenylacetylene (2.0 g, 20 mmol) and Et_3N (4.5 g, 45 mmol) in 1,4-dioxane (50 mL) at rt under nitrogen were added $[1,1'$ -bis(diphenylphosphino)ferrocene]dichloro-palladium(II) (0.73 g, 1 mmol) and CuI (0.75 g, 4 mmol). The mixture was stirred at 80 °C for 2 h and then cooled to rt, and the solvent was evaporated in vacuo. The resulting residue was dissolved in EtOAc and washed with H_2O . The organic layer was separated, dried (Na_2SO_4), and filtered, and the solvent was evaporated in vacuo. The crude product was purified by flash column chromatography (silica gel, EtOAc in petroleum ether, 10/90 to 50/50). The desired fractions were collected, and the solvent was evaporated in vacuo to yield 0.7 g (30%) of **14a** as a brown solid. Mp^a 232.1–235.1 °C. 1H NMR (400 MHz, DMSO- d_6) δ ppm 3.00 (t, $J = 7.0$ Hz, 2 H), 3.50 (td, $J = 7.0, 2.5$ Hz, 2 H), 7.44–7.57 (m, 3 H), 7.63–7.72 (m, 2 H), 8.07 (br. s, 1 H). LCMS: m/z 255 $[M + H]^+$, $t_R = 5.00$ min.

5-Methyl-2-phenylethynyl-6,7-dihydro-5H-thiazolo[5,4-*c*]pyridin-4-one (14b). A mixture of **14a** (0.25 g, 0.98 mmol), methyl iodide (0.84 g, 5.9 mmol), and Cs_2CO_3 (1.9 g, 5.9 mmol) in CH_3CN (50 mL) was stirred at 80 °C for 16 h. The mixture was then cooled to rt and concentrated in vacuo. The crude product was purified by reverse phase HPLC (0.1% TFA in CH_3CN /0.1% TFA in H_2O). The desired fractions were collected, washed with a saturated solution of $NaHCO_3$ and extracted with EtOAc. The organic layer was separated, dried (Na_2SO_4), and filtered, and the solvent was evaporated in vacuo to yield 50 mg (19%) of **14b**. Mp^a 146.1–147.2 °C. 1H NMR (400 MHz,

DMSO- d_6) δ ppm 2.97 (s, 3 H), 3.09 (t, J = 7.2 Hz, 2 H), 3.67 (t, J = 7.2 Hz, 2 H), 7.43–7.58 (m, 3 H), 7.67 (d, J = 6.8 Hz, 2 H). LCMS: m/z 269 $[M + H]^+$, t_R = 5.29 min.

5-(2-Methoxy-ethyl)-2-phenylethynyl-6,7-dihydro-5H-thiazolo[5,4-c]pyridin-4-one (14c). Starting from **14a** (0.7 g, 2.9 mmol) and 2-bromoethyl methyl ether and following the procedure described for **14b**, **14c** was obtained as a yellow solid (150 mg, 20%). M_p^a 144.5–148.2 °C. 1H NMR (300 MHz, $CDCl_3$) δ ppm 3.06 (t, J = 7.0 Hz, 2 H), 3.30 (s, 3 H), 3.49–3.59 (m, 2 H), 3.59–3.68 (m, 2 H), 3.74 (t, J = 7.0 Hz, 2 H), 7.26–7.43 (m, 3 H), 7.45–7.62 (m, 2 H). LCMS: m/z 313 $[M + H]^+$, t_R = 6.01 min.

2-Benzyloxy-6,7-dihydro-5H-thiazolo[5,4-c]pyridin-4-one (15a). Benzyl alcohol (0.145 mL, 1.42 mmol) was added dropwise to a suspension of NaH (0.067 g, 1.67 mmol, 60% in mineral oils) in THF (6 mL) under nitrogen. The mixture was stirred at rt for 15 min and then **21** (0.3 g, 1.29 mmol) was added. The mixture was stirred at 120 °C for 15 min under microwave irradiation in a sealed tube. The solvent was removed with a nitrogen flow to yield 0.340 g (70% pure) of **15a**. LCMS: m/z 261 $[M + H]^+$, t_R = 2.15 min.

2-Benzyloxy-5-methyl-6,7-dihydro-5H-thiazolo[5,4-c]pyridin-4-one (15b). **15a** (0.34 g, 1.29 mmol) was added dropwise to a suspension of NaH (0.067 g, 1.67 mmol, 60% in mineral oils) in THF (2 mL) under nitrogen. The mixture was stirred for 15 min then methyl iodide (0.12 mL, 1.68 mmol). The mixture was stirred at 120 °C for 15 min under microwave irradiation in a sealed tube. The mixture was diluted with EtOAc and washed with a saturated solution of NH_4Cl . The organic layer was separated, dried (Na_2SO_4), and filtered, and the solvent was evaporated in vacuo. The crude product was purified by flash column chromatography (silica gel, EtOAc in CH_2Cl_2 , 0/100 to 10/90). The desired fractions were collected and the solvents evaporated in vacuo. The solid obtained was triturated with heptane/Et₂O to yield 0.190 g (54%) of **15b**. M_p^b 106.4 °C. 1H NMR (500 MHz, $CDCl_3$) δ ppm 2.96 (t, J = 7.2 Hz, 2 H), 3.05 (s, 3 H), 3.60 (t, J = 7.2 Hz, 2 H), 5.45 (s, 2 H), 7.34–7.50 (m, 5 H). LCMS: m/z 275 $[M + H]^+$, t_R = 1.68 min.

2-Benzyloxy-5-(4-fluoro-phenyl)-6,7-dihydro-5H-thiazolo[5,4-c]pyridin-4-one (15c). Benzyl alcohol (0.38 mL, 3.67 mmol) was added dropwise to a suspension of NaH (0.183 g, 4.58 mmol, 60% in mineral oils) in THF (12 mL) under nitrogen. The mixture was stirred at rt for 15 min and then **26** (1 g, 3.06 mmol) was added. The mixture was stirred at 120 °C for 25 min under microwave irradiation in a sealed tube. The mixture was partitioned between CH_2Cl_2 and H_2O . The organic layer was separated, dried ($MgSO_4$), and filtered, and the solvent was evaporated in vacuo. The crude product was purified by flash column chromatography (silica gel, EtOAc in CH_2Cl_2 in heptane, 0/0/100 to 10/10/80). The desired fractions were collected and evaporated in vacuo to yield 0.68 g (63%) of **15c** as a white solid. M_p^b 130.0 °C. 1H NMR (400 MHz, $CDCl_3$) δ ppm 3.08 (t, J = 6.9 Hz, 2 H), 4.01 (t, J = 6.9 Hz, 2 H), 5.49 (s, 2 H), 7.08 (t, J = 8.7 Hz, 2 H), 7.29 (dd, J = 9.0, 4.9 Hz, 2 H), 7.34–7.54 (m, 5 H). ^{13}C NMR (126 MHz, $CDCl_3$) δ ppm 26.56 (s, 1 C) 49.57 (s, 1 C) 73.78 (s, 1 C) 115.68 (d, J = 22.00 Hz, 2 C) 119.25 (s, 1 C) 127.02 (d, J = 8.25 Hz, 2 C) 128.32 (s, 2 C) 128.64 (s, 2 C) 128.78 (s, 1 C) 134.65 (s, 1 C) 138.24 (d, J = 3.67 Hz, 1 C) 155.14 (s, 1 C) 160.62 (d, J = 245.61 Hz, 1 C) 160.68 (s, 1 C) 177.92 (s, 1 C). LCMS: m/z 355 $[M+H]^+$, t_R = 2.44 min. HRMS (ES^+ , $M + H$) calcd. for $C_{19}H_{16}N_2O_2SF$: 355.0917, found 355.0914.

5-Methyl-2-phenoxymethyl-6,7-dihydro-5H-thiazolo[5,4-c]pyridin-4-one (16a). Di-*tert*-butyl azodicarboxylate (1.55 g, 5.90 mmol) was added to a stirred solution of **29** (0.90 g, 4.54 mmol), phenol (0.534 g, 5.68 mmol) and PPh_3 (1.55 g, 5.90 mmol) in THF (15 mL) under nitrogen. The mixture was stirred at 120 °C for 20 min under microwave irradiation. The solvent was evaporated in vacuo. The crude product was purified by flash column chromatography (silica gel, EtOAc in CH_2Cl_2 , 0/100 to 50/50). The desired fractions were collected and evaporated in vacuo, and the residue was triturated with diisopropyl ether to yield 0.253 g (20%) of **16a** as a white solid. M_p^a 141.5–142.4 °C. 1H NMR (500 MHz, $CDCl_3$) δ ppm 3.10 (s, 3 H), 3.14 (t, J = 7.2 Hz, 2 H), 3.67 (t, J = 7.1 Hz, 2 H), 5.33 (s, 2 H), 6.96–7.05 (m, 3 H), 7.28–7.35 (m, 2 H). ^{13}C NMR (126 MHz,

$CDCl_3$) δ ppm 25.64 (s, 1 C) 34.14 (s, 1 C) 48.56 (s, 1 C) 67.30 (s, 1 C) 114.85 (s, 2 C) 121.89 (s, 1 C) 127.04 (s, 1 C) 129.56 (s, 2 C) 157.41–157.65 (m, 1 C) 157.69–157.96 (m, 1 C) 160.76–161.07 (m, 1 C) 171.74 (s, 1 C). LCMS: m/z 275 $[M + H]^+$, t_R = 1.76 min. HRMS (ES^+ , $M + H$) calcd. for $C_{14}H_{13}N_2O_2S$: 275.0854, found 275.0853.

5-Ethyl-2-phenoxymethyl-6,7-dihydro-5H-thiazolo[5,4-c]pyridin-4-one (16b). Iodoethane (0.069 mL, 0.86 mmol) was added to a suspension of **31** (150 mg, 0.058 mmol) and CS_2CO_3 (281 mg, 0.86 mmol) in anhydrous DMF (2.5 mL). The mixture was stirred at rt for 16 h under nitrogen then at 100 °C for 1 h. The mixture was diluted with H_2O and extracted with EtOAc. The organic layer was separated, washed with brine, dried (Na_2SO_4), and filtered, and the solvents were evaporated in vacuo. The crude product was purified by flash column chromatography (silica gel, EtOAc in CH_2Cl_2 , 0/100 to 50/50). The desired fractions were collected and the solvents evaporated in vacuo. The impure product was triturated with diisopropyl ether and purified by reverse phase HPLC (gradient elution: 80% 0.1% NH_4CO_3H/NH_4OH pH 9 solution in H_2O , 20% CH_3CN to 0% 0.1% NH_4CO_3H/NH_4OH pH 9 solution in H_2O , 100% CH_3CN). The desired fractions were collected and evaporated in vacuo to yield 62 mg (37%) of **16b** as a yellow solid. M_p^b 116.0 °C. 1H NMR (400 MHz, $CDCl_3$) δ ppm 1.21 (t, J = 7.2 Hz, 3 H), 3.12 (t, J = 7.1 Hz, 2 H), 3.57 (q, J = 7.2 Hz, 2 H), 3.67 (t, J = 7.2 Hz, 2 H), 5.33 (s, 2 H), 6.95–7.07 (m, 3 H), 7.28–7.36 (m, 2 H). ^{13}C NMR (101 MHz, $CDCl_3$) δ ppm 12.79 (s, 1 C) 25.90 (s, 1 C) 41.35 (s, 1 C) 45.97 (s, 1 C) 67.30 (s, 1 C) 114.87 (s, 2 C) 121.92 (s, 1 C) 127.46 (s, 1 C) 129.61 (s, 2 C) 157.54 (s, 1 C) 157.82 (s, 1 C) 160.31 (s, 1 C) 171.75 (s, 1 C). LCMS: m/z 289 $[M + H]^+$, t_R = 2.00 min. HRMS (ES^+ , $M + H$) calcd. for $C_{15}H_{17}N_2O_2S$: 289.1011, found 289.1013.

5-Isopropyl-2-phenoxymethyl-6,7-dihydro-5H-thiazolo[5,4-c]pyridin-4-one (16c). A mixture of **25a** (0.23 g, 1.29 mmol) and **33a** (0.24 g, 1.4 mmol) in EtOH (10 mL) was stirred at rt for 15 min before $NaHCO_3$ (0.4 g, 3.9 mmol) was added. Then the mixture was stirred at 70 °C for 15 min, diluted with EtOAc, and washed with H_2O . The organic layer was separated, washed with brine, dried (Na_2SO_4), and filtered, and the solvents were evaporated in vacuo. The crude product was purified by reverse phase HPLC (gradient elution: 0.1% TFA in CH_3CN /0.1% TFA in H_2O). The desired fractions were collected and washed with a saturated solution of $NaHCO_3$ and extracted with EtOAc (2 \times 100 mL). The organic layer was separated, washed with brine, dried (Na_2SO_4), filtered and the solvents evaporated in vacuo to yield 81 mg (21%) of **16c** as a white solid. M_p^a 104.1–106.0 °C. 1H NMR (400 MHz, $CDCl_3$) δ ppm 1.13 (d, J = 6.8 Hz, 6 H), 3.00 (t, J = 7.0 Hz, 2 H), 3.49 (t, J = 7.0 Hz, 2 H), 4.87 (spt, J = 6.8 Hz, 1 H), 5.26 (s, 2 H), 6.86–7.01 (m, 3 H), 7.21–7.31 (m, 2 H). LCMS: m/z 303 $[M + H]^+$, t_R = 5.42 min.

5-(2-Methoxy-ethyl)-2-phenoxymethyl-6,7-dihydro-5H-thiazolo[5,4-c]pyridin-4-one (16d). Starting from **31** (150 mg, 0.58 mmol) and 2-bromoethyl methyl ether and following the procedure described for **16b**, **16d** was obtained as a yellow solid (90 mg, 49%). M_p^b 82.6 °C. 1H NMR (500 MHz, $CDCl_3$) δ ppm 3.10 (t, J = 7.1 Hz, 2 H), 3.36 (s, 3 H), 3.60 (t, J = 5.2 Hz, 2 H), 3.69 (t, J = 5.2 Hz, 2 H), 3.78 (t, J = 7.2 Hz, 2 H), 5.33 (s, 2 H), 6.97–7.04 (m, 3 H), 7.28–7.35 (m, 2 H). LCMS: m/z 319 $[M + H]^+$, t_R = 1.90 min.

5-Cyclopropyl-2-phenoxymethyl-6,7-dihydro-5H-thiazolo[5,4-c]pyridin-4-one (16e). Starting from **25b** (0.28 g, 1.2 mmol) and **33a** (0.23 g, 1.4 mmol) and following the procedure described for **16c**, **16e** was obtained as a white solid (72 mg, 20%). M_p^a 252.1–255.3 °C. 1H NMR (400 MHz, $CDCl_3$) δ ppm 0.62–0.69 (m, 2 H), 0.80–0.88 (m, 2 H), 2.65 (tt, J = 7.2, 3.7 Hz, 1 H), 2.99 (t, J = 7.0 Hz, 2 H), 3.63 (t, J = 7.0 Hz, 2 H), 5.25 (s, 2 H), 6.89–6.99 (m, 3 H), 7.21–7.29 (m, 2 H). LCMS: m/z 301 $[M + H]^+$, t_R = 4.86 min.

5-Cyclopropylmethyl-2-phenoxymethyl-6,7-dihydro-5H-thiazolo[5,4-c]pyridin-4-one (16f). Starting from **25c** (250 mg, 1.01 mmol) and **33a** (0.2 g, 1.22 mmol) and following the procedure described for **16c**, **16f** was obtained as a white solid (78 mg, 25%). M_p^a 292.6–302.9 °C. 1H NMR (400 MHz, $CDCl_3$) δ ppm 0.23 (q, J = 4.9 Hz, 2 H), 0.40–0.56 (m, 2 H), 0.87–1.06 (m, 1 H), 3.08 (t, J = 7.2 Hz, 2 H), 3.35 (d, J = 7.0 Hz, 2 H), 3.72 (t, J = 7.2 Hz, 2 H), 5.28 (s, 2 H), 6.86–7.02 (m, 3 H), 7.21–7.33 (m, 2 H). ^{13}C NMR (101 MHz,

CDCl_3) δ ppm 3.49 (s, 2 C) 9.53 (s, 1 C) 25.89 (s, 1 C) 46.52 (s, 1 C) 50.68 (s, 1 C) 67.32 (s, 1 C) 114.89 (s, 2 C) 121.93 (s, 1 C) 127.46 (s, 1 C) 129.62 (s, 2 C) 157.55 (s, 1 C) 157.85 (s, 1 C) 160.56 (s, 1 C) 171.80 (s, 1 C). LCMS: m/z 303 $[\text{M} + \text{H}]^+$, t_R = 5.32 min. HRMS (ES^+ , $\text{M} + \text{H}$) calcd. for $\text{C}_{17}\text{H}_{19}\text{N}_2\text{O}_2\text{S}$: 315.1167, found 315.1169.

2-Phenoxymethyl-5-(tetrahydro-pyran-4-ylmethyl)-6,7-dihydro-5H-thiazolo[5,4-c]pyridin-4-one (16g). Starting from **31** (150 mg, 0.58 mmol) and 4-(bromomethyl)tetrahydropyran and following the procedure described for **16a**, **16g** was obtained as a white solid (27 mg, 13%). ^1H NMR (400 MHz, CDCl_3) δ ppm 1.34–1.48 (m, 2 H), 1.59–1.68 (m, 2 H), 1.90–2.04 (m, 1 H), 3.11 (t, J = 7.0 Hz, 2 H), 3.32–3.42 (m, 2 H), 3.40 (d, J = 7.4 Hz, 2 H), 3.69 (t, J = 7.0 Hz, 2 H), 3.94–4.03 (m, 2 H), 5.33 (s, 2 H), 6.97–7.05 (m, 3 H), 7.28–7.35 (m, 2 H). LCMS: m/z 359 $[\text{M} + \text{H}]^+$, t_R = 2.10 min.

5-(4-Fluoro-phenyl)-2-phenoxymethyl-6,7-dihydro-5H-thiazolo[5,4-c]pyridin-4-one (16h). A mixture of **25d** (0.41 g, 1.45 mmol) and **33a** (0.22 g, 1.3 mmol) in DMF (5 mL) was stirred at rt for 15 min before NaHCO_3 (0.19 g, 2.3 mmol) was added. Then the mixture was stirred at 100 °C for 30 min, diluted with EtOAc and washed with H_2O . The organic layer was separated, dried (MgSO_4), and filtered, and the solvents were evaporated in vacuo. The crude product was purified by flash column chromatography (silica gel, EtOAc in CH_2Cl_2 , 0/100 to 2/98). The desired fractions were collected, and the solvents were evaporated in vacuo to yield 0.084 g (16%) of **16h** as a white solid. Mp^b 163.3 °C. ^1H NMR (500 MHz, CDCl_3) δ ppm 3.26 (t, J = 6.9 Hz, 2 H), 4.08 (t, J = 6.9 Hz, 2 H), 5.36 (s, 2 H), 6.98–7.06 (m, 3 H), 7.07–7.13 (m, 2 H), 7.28–7.36 (m, 4 H). ^{13}C NMR (126 MHz, CDCl_3) δ ppm 26.32 (s, 1 C) 50.16 (s, 1 C) 67.37 (s, 1 C) 114.87 (s, 2 C) 115.82 (d, J = 22.91 Hz, 2 C) 122.01 (s, 1 C) 127.15 (d, J = 8.25 Hz, 2 C) 127.38 (s, 1 C) 129.64 (s, 2 C) 137.93 (d, J = 3.67 Hz, 1 C) 157.50 (s, 1 C) 158.79 (s, 1 C) 160.79 (d, J = 246.52 Hz, 1 C) 160.36 (s, 1 C) 172.95 (s, 1 C). LCMS: m/z 355 $[\text{M} + \text{H}]^+$, t_R = 6.57 min. HRMS (ES^+ , $\text{M} + \text{H}$) calcd. for $\text{C}_{19}\text{H}_{16}\text{N}_2\text{O}_2\text{SF}$: 355.0917, found 355.0916.

5-(2,4-Difluoro-phenyl)-2-phenoxymethyl-6,7-dihydro-5H-thiazolo[5,4-c]pyridin-4-one (16i). Starting from **25e** (300 mg, 0.99 mmol) and **33a** (148 mg, 0.89 mmol) and following the procedure described for **16h**, **16i** was obtained as a yellow solid (37 mg, 10%). Mp^a 268.9–284.1 °C. ^1H NMR (400 MHz, CDCl_3) δ ppm 3.28 (t, J = 6.9 Hz, 2 H), 4.01 (t, J = 6.8 Hz, 2 H), 5.37 (s, 2 H), 6.89–6.99 (m, 2 H), 6.99–7.07 (m, 3 H), 7.29–7.39 (m, 3 H). LCMS: m/z 373 $[\text{M} + \text{H}]^+$, t_R = 5.63 min.

2-(2-Fluoro-phenoxymethyl)-5-(4-fluoro-phenyl)-6,7-dihydro-5H-thiazolo[5,4-c]pyridin-4-one (16j). A mixture of **35** (0.3 g, 1.01 mmol), 2-fluorophenol (0.15 g, 1.3 mmol) and K_2CO_3 (0.4 g, 3 mmol) in DMF (40 mL) was stirred at rt for 1 h. The mixture was filtered and the solvent evaporated in vacuo. The crude product was purified by reverse phase HPLC (gradient elution: 0.1% TFA in $\text{CH}_3\text{CN}/0.1\%$ TFA in H_2O). The desired fractions were collected and washed with a saturated solution of NaHCO_3 and extracted with EtOAc (2 \times 100 mL). The organic layer was separated, dried (Na_2SO_4), filtered and the solvent evaporated in vacuo to yield 31 mg (8%) of **16j** as a solid. Mp^a > 280 °C. ^1H NMR (300 MHz, CDCl_3) δ ppm 3.25 (t, J = 6.9 Hz, 2 H), 4.07 (t, J = 6.8 Hz, 2 H), 5.41 (s, 2 H), 6.92–7.19 (m, 6 H), 7.19–7.42 (m, 2 H). LCMS: m/z 373 $[\text{M} + \text{H}]^+$, t_R = 4.58 min.

2-(3-Fluoro-phenoxymethyl)-5-(4-fluoro-phenyl)-6,7-dihydro-5H-thiazolo[5,4-c]pyridin-4-one (16k). Starting from **25d** (0.39 g, 1.38 mmol) and **33b** (230 mg, 1.24 mmol) and following the procedure described for **16h**, **16k** was obtained as a white solid (120 mg, 23%). Mp^b 152.8 °C. ^1H NMR (500 MHz, CDCl_3) δ ppm 3.27 (t, J = 6.9 Hz, 2 H), 4.09 (t, J = 6.9 Hz, 2 H), 5.35 (s, 2 H), 6.69–6.84 (m, 2 H), 7.07–7.16 (m, 2 H), 7.23–7.35 (m, 4 H). LCMS: m/z 372 $[\text{M} + \text{H}]^+$, t_R = 2.88 min.

2-(4-Fluoro-phenoxymethyl)-5-(4-fluoro-phenyl)-6,7-dihydro-5H-thiazolo[5,4-c]pyridin-4-one (16l). Starting from **35** (0.3 g, 1.01 mmol) and 4-fluorophenol (0.15 g, 1.3 mmol) and following the procedure described for **16j**, **16l** was obtained as a solid (74 mg, 20%). Mp^a > 280 °C. ^1H NMR (300 MHz, CDCl_3) δ ppm 3.25 (t, J = 6.7 Hz, 2 H), 4.07 (t, J = 6.8 Hz, 2 H), 5.31 (s, 2 H), 6.85–7.05 (m, 4 H),

7.09 (br. t, J = 8.4, 8.4 Hz, 2 H), 7.26–7.35 (m, 2 H). LCMS: m/z 373 $[\text{M} + \text{H}]^+$, t_R = 4.62 min.

2-Phenoxymethyl-5-pyridin-2-yl-6,7-dihydro-5H-thiazolo[5,4-c]pyridin-4-one (16m). K_2CO_3 (111 mg, 0.81 mmol) was added to a stirred suspension of **31** (150 mg, 0.4 mmol), 2-iodopyridine (0.043 mL, 0.4 mmol), CuI (0.015 g, 0.081 mmol) and N,N' -dimethylethylenediamine (0.026 mL, 0.24 mmol) in toluene (3 mL) in a sealed tube and under nitrogen. The mixture was stirred at 120 °C for 16 h, filtered through a Celite pad, and washed with EtOAc and the filtrate was evaporated in vacuo. The crude product was purified by flash column chromatography (silica gel, EtOAc in CH_2Cl_2 , 0/100 to 100/0). The desired fractions were collected and the solvents were evaporated in vacuo. The solid was triturated with diisopropyl ether to yield 57 mg (57%) of **16m** as a white solid. Mp^b 143.9 °C. ^1H NMR (400 MHz, CDCl_3) δ ppm 3.23 (t, J = 6.8 Hz, 2 H), 4.47 (t, J = 6.8 Hz, 2 H), 5.37 (s, 2 H), 7.00–7.06 (m, 3 H), 7.07–7.13 (m, 1 H), 7.29–7.37 (m, 2 H), 7.71 (ddd, J = 8.6, 7.1, 1.8 Hz, 1 H), 7.89 (d, J = 8.3 Hz, 1 H), 8.44 (br. s, 1 H). LCMS: m/z 338 $[\text{M} + \text{H}]^+$, t_R = 2.42 min.

2-Phenoxymethyl-5-pyridin-3-yl-6,7-dihydro-5H-thiazolo[5,4-c]pyridin-4-one (16n). Starting from **31** (150 mg, 0.58 mmol) and 3-bromopyridine and following the procedure described for **16m**, **16n** was obtained as a white solid (29 mg, 15%). ^1H NMR (400 MHz, CDCl_3) δ ppm 3.30 (t, J = 6.8 Hz, 2 H), 4.17 (t, J = 6.8 Hz, 2 H), 5.37 (s, 2 H), 6.96–7.09 (m, 3 H), 7.29–7.41 (m, 3 H), 7.71–7.80 (m, 1 H), 8.50 (dd, J = 4.7, 1.3 Hz, 1 H), 8.65 (d, J = 2.3 Hz, 1 H). LCMS: m/z 338 $[\text{M} + \text{H}]^+$, t_R = 2.00 min.

2-Phenoxymethyl-5-pyridin-4-yl-6,7-dihydro-5H-thiazolo[5,4-c]pyridin-4-one (16o). Starting from **31** (150 mg, 0.58 mmol) and 4-iodopyridine and following the procedure described for **16m**, **16o** was obtained as a white solid (5 mg, 2.5%). ^1H NMR (500 MHz, CDCl_3) δ ppm 3.29 (t, J = 6.8 Hz, 2 H), 4.19 (t, J = 6.8 Hz, 2 H), 5.37 (s, 2 H), 6.90–7.12 (m, 3 H), 7.29–7.41 (m, 4 H), 8.62 (d, J = 6.4 Hz, 2 H). LCMS: m/z 338 $[\text{M} + \text{H}]^+$, t_R = 2.09 min.

5-(5-Fluoro-pyridin-2-yl)-2-phenoxymethyl-6,7-dihydro-5H-thiazolo[5,4-c]pyridin-4-one (16p). K_3PO_4 (1.6 g, 7.49 mmol) was added to a stirred suspension of **31** (650 mg, 2.5 mmol), 2-bromo-5-fluoropyridine (879 mg, 4.99 mmol), CuI (475 mg, 2.5 mmol) and N,N' -dimethylethylenediamine (0.81 mL, 7.49 mmol) in toluene (12 mL) in a sealed tube and under nitrogen. The mixture was stirred at 140 °C for 16 h and then filtered through a Celite pad. The filtrate was evaporated in vacuo. The crude product was purified by flash column chromatography (silica gel, EtOAc in CH_2Cl_2 , 0/100 to 30/70). The desired fractions were collected and the solvents evaporated in vacuo. The solid was triturated with diisopropyl ether to yield 570 mg (64%) of **16p** as a white solid. Mp^a 131.7–132.8 °C. ^1H NMR (500 MHz, CDCl_3) δ ppm 3.23 (t, J = 6.8 Hz, 2 H), 4.42 (t, J = 6.9 Hz, 2 H), 5.37 (s, 2 H), 6.86–7.12 (m, 3 H), 7.29–7.38 (m, 2 H), 7.39–7.50 (m, 1 H), 7.89 (dd, J = 9.2, 4.0 Hz, 1 H), 8.27 (d, J = 3.2 Hz, 1 H). ^{13}C NMR (101 MHz, CDCl_3) δ ppm 26.15 (s, 1 C) 46.39 (s, 1 C) 67.41 (s, 1 C) 114.83 (s, 2 C) 120.72 (d, J = 4.24 Hz, 1 C) 122.02 (s, 2 C) 124.21 (d, J = 19.78 Hz, 1 C) 127.41 (s, 1 C) 129.65 (s, 2 C) 134.92 (d, J = 25.43 Hz, 1 C) 149.26 (d, J = 2.12 Hz, 1 C) 158.76 (d, J = 259.96 Hz, 1 C) 157.89 (s, 1 C) 160.67 (s, 1 C) 173.65 (s, 1 C). LCMS: m/z 356 $[\text{M} + \text{H}]^+$, t_R = 5.99 min. HRMS (ES^+ , $\text{M} + \text{H}$) calcd. for $\text{C}_{18}\text{H}_{15}\text{N}_3\text{O}_2\text{SF}$: 356.0869, found 356.0870.

5-(3-Fluoro-pyridin-2-yl)-2-phenoxymethyl-6,7-dihydro-5H-thiazolo[5,4-c]pyridin-4-one (16q). Starting from **31** (150 mg, 0.58 mmol) and 2-chloro-3-fluoropyridine and following the procedure described for **16m**, **16q** was obtained as a white solid (22 mg, 15%). ^1H NMR (400 MHz, CDCl_3) δ ppm 3.29 (t, J = 6.8 Hz, 2 H), 4.25 (t, J = 6.8 Hz, 2 H), 5.38 (s, 2 H), 6.98–7.06 (m, 3 H), 7.23–7.29 (m, 1 H), 7.30–7.40 (m, 2 H), 7.51 (ddd, J = 9.7, 8.1, 1.6 Hz, 1 H), 8.31 (dt, J = 4.8, 1.2 Hz, 1 H). LCMS: m/z 356 $[\text{M} + \text{H}]^+$, t_R = 2.37 min.

Biology. Cell Culture. Human embryonic kidney (HEK) 293 cells were stably transfected with human mGluR_{5a} cDNA in expression vector pcDNA4/TO. hmGlu₅ receptor-expressing HEK293 cells were maintained in Dulbecco's modified Eagle's medium (DMEM) supplemented with 10% heat inactivated dialyzed fetal bovine serum and antibiotics (88 IU/mL penicillin G and 88 $\mu\text{g}/\text{mL}$ streptomycin

sulfate). Cells were detached with PBS w/o $\text{Ca}^{2+}/\text{Mg}^{2+}$ containing 0.04% EDTA and 0.005% trypsin. The cells were grown in 175 cm^2 culture flasks at 37 °C in a 5% CO_2 environment and held under permanent selection with 200 $\mu\text{g}/\text{mL}$ zeocin and 5 $\mu\text{g}/\text{mL}$ blasticidin. Cells were cultured at 40 000 cells/ cm^2 or 20 000 cells/ cm^2 for respectively 3 or 4 days of growth in a F175 flask.

Calcium Mobilization Assay. Cells were seeded at 40 000 cells/well in PDL-coated MW384, and a day later, medium was removed before addition of a fluo-4-AM solution (HBSS, 2.5 mM probenecid and ~2 μM fluo-4-AM, pH 7.4). Measurements were performed 90 min later (while incubation at 37 °C and 5% CO_2) using the FDSS. Two additions were made: first, compound alone was added at 6 s to detect any agonist activity. Next, a suboptimal concentration (nominally 20% of the maximum response, EC_{20}) of glutamate was added at 157 s to detect any potentiation of the glutamate response. For each interval, Ca^{2+} fluorescence of the Ca^{2+} -bound dye was monitored every second, at an excitation wavelength of 480 nm and emission at 540 nm. The ratio of peak versus basal fluorescent signals was used for data analysis.

Data Analysis. Data were normalized to the control agonist response and sigmoid concentration–response curves plotting these percentages versus the log concentration of the test compound were analyzed using a 4 parameter logistic nonlinear regression model programmed in R (R Development Core Team, 2010. R: A language and environment for statistical computing. R Foundation for Statistical Computing, Vienna, Austria. ISBN 3–900051–07–0, URL <http://www.R-project.org/>). The model was determined by the maximal effect of each compound (E_{max}), its EC_{50} and the response in the absence of compound. The fourth parameter determining the slope was fixed to 1. In addition, the heterogeneity between experiments and concentration–response curves for each compound was taken into account by the inclusion of a random effect in both ' E_0 ' (response in the absence of compound) and E_{max} of the model.

In Vivo Pharmacology. (a) *Animal Husbandry.* Animals were housed in the animal care facility certified by the American Association for the Accreditation of Laboratory Animal Care (AAALAC) under a 12-h light/dark cycle (lights on: 7 a.m.; lights off: 7 p.m.) and had free access to food and water. The animals used in these experiments were food-deprived the evening before experimentation for oral administration of test compound. The experimental protocols performed during the light cycle were approved by the Institutional Animals Care and Use Committee of Vanderbilt University and conformed to the guidelines established by the National Research Council Guide for the Care and Use of Laboratory Animals.

(b) *Preparation of Test Article.* **16a** was formulated in volumes specific to the number of animals dosed each day. The solutions were formulated so that animals were injected with a maximal dosing volume of 10 mL/kg. The appropriate amount according to the dosage was mixed into a 20% 2-(hydroxypropyl)- β -cyclodextrin in sterile water (HP- β -CD; Sigma, Cat. No. C0926-10G) solution. Each mixture was ultrahomogenized on ice for 2–3 min using a hand-held tissue homogenizer. Next, the pH of all solutions was checked using 0–14 EMD pH strips and adjusted to a pH of 6–7 if necessary with 1N NaOH. The mixtures were then vortexed, and stored in a sonication bath at 40 °C until time of injection. *d*-Amphetamine hemisulfate (AMP) was obtained from Sigma (Cat. No. A5880-1G; St. Louis, MO). Salt-correction was used to determine the correct amount of the *d*-amphetamine hemisulfate form in mg to add to sterile water in order to yield a 1 mg/mL solution; injected with a maximal dosing volume of 10 mL/kg.

Reversal of Amphetamine-Induced Hyperlocomotion. Studies were conducted using Smart Open Field activity chambers (27 × 27 × 20 cm) (Kinder Scientific, Poway, CA) equipped with 16 horizontal (x- and y-axes) infrared photobeams. Changes in locomotor activity were measured as the number of photobeam breaks over time and were recorded with a Pentium I computer equipped with rat activity monitoring system software (Motor Monitor, Kinder Scientific, Poway, CA). Male Harlan Sprague–Dawley rats (Harlan Laboratories, Indianapolis, IN) weighing 250–375 g were used. Animals were habituated in the locomotor activity test chambers for 30 min. Animals were next pretreated for an additional 30 min with either vehicle or a

dose of **16a** p.o., followed by a subcutaneous injection of 1 mg/kg amphetamine or vehicle and monitored for an additional 60 min. **Treatment groups.** Dose group 1: VAMP = 20% β -CD (**16a** vehicle), p.o. + 1 mg/kg AMP, sc ($n = 8$). Dose group 2: 3AMP = 3 mg/kg **16a**, p.o. + 1 mg/kg AMP, sc ($n = 6$). Dose group 3: 10AMP = 10 mg/kg **16a**, p.o. + 1 mg/kg AMP, sc ($n = 7$). Dose group 4: 30AMP = 30 mg/kg **16a**, p.o. + 1 mg/kg AMP, sc ($n = 8$). Dose group 5: 56.6AMP = 56.6 mg/kg **16a**, p.o. + 1 mg/kg AMP, sc ($n = 8$). Dose group 6: 100AMP = 100 mg/kg **16a**, p.o. + 1 mg/kg AMP, sc ($n = 8$). Dose group 7: 100 V = 100 mg/kg **16a**, p.o. + sterile water (AMP vehicle), sc ($n = 8$). Changes in locomotor activity were recorded for a total of 120 min. Data were expressed as changes in ambulation defined as the total number of photobeam breaks per 5 min interval. At the end of this behavioral study, each animal was euthanized, then decapitated, and the plasma and brain tissues were collected for the evaluation of exposure levels of **16a**. **Data Analysis.** Behavioral data were analyzed using a one-way ANOVA with main effects of treatment and time. *Post hoc* analyses were performed using a Dunnett's *t*-test with all treatment groups compared to the VAMP group using JMP 8.0 (SAS Institute, Cary, NC) statistical software. Data were graphed using SigmaPlot for Windows Version 11.0 (Saugua, MA). A probability of $p \leq 0.05$ was taken as the level of statistical significance. Percent Effect and Reversal calculations for the 3AMP, 10AMP, 30AMP, 56.6AMP, and 100AMP treatment groups were performed with the following formula relative to the VAMP treatment group: (1) Total number of photobeam breaks in the time interval from $t = 60$ to $t = 120$ was calculated for each rat in each treatment group; (2) Mean total number of photobeam breaks in the time interval from $t = 60$ to $t = 120$ was calculated for the VAMP group; (3) Percent effect = ratio of the total number of photobeam breaks for each rat in each treatment group divided by the mean total number of photobeam breaks in the time interval from $t = 60$ to $t = 120$ of the VAMP group multiplied by 100; (4) Percent reversal = 100-the percent effect for each rat in each treatment group; (5) finally the mean \pm SE percent reversal for each treatment group was calculated from the individual percent reversal values. Percent effect and change calculations for the VAMP and 100 V treatment groups relative to the VV treatment group were also performed with the following formula: (1) Total number of photobeam breaks in the time interval from $t = 60$ to $t = 120$ was calculated for each rat in each treatment group; (2) Mean total number of photobeam breaks in the time interval from $t = 60$ to $t = 120$ was calculated for the VV group; (3) Percent Effect = Ratio of the total number of photobeam breaks for each rat in each treatment group divided by the mean total number of photobeam breaks in the time interval from $t = 60$ to $t = 120$ of the VV group multiplied by 100; (4) percent change = the percent effect for each rat in each treatment group –100; (5) finally the Mean \pm SE percent change for each treatment group was calculated from the individual percent change values. **LC-MS/MS Sample Preparation and Analysis Methodology.** Brain samples were homogenized in 3 mL of 70:30 isopropanol/water and then centrifuged at 3500 rpm for 5 min. Resulting brain sample supernatant and plasma samples were transferred into a 96-well plate containing plasma blanks, plasma double blank, a standard curve of the test article, and quality control samples for subsequent LC-MS/MS analysis. Each sample was diluted with acetonitrile containing 50 nM carbamazepine (internal standard), centrifuged at 3500 rpm, and the resulting supernatant was transferred to a new 96-well plate. After an equal volume of water was added to each sample (to provide 50:50 acetonitrile/water solution), the plate was analyzed via ESI on a triple-quadrupole mass spectrometer (AB Sciex API-4000) coupled with an autosampling liquid chromatography system (Shimadzu LC-10AD pumps, Leap Technologies CTC PAL autosampler). Analyte (test article) was separated by gradient elution using a C18 3.0 × 50 mm, 3 μm column (Fortis Technologies) thermostatted at 40 °C. HPLC mobile phase A was 0.1% formic acid in water (pH unadjusted), mobile phase B was 0.1% formic acid in acetonitrile (pH unadjusted), and the gradient used was 30–90% mobile phase B with 0.2 min hold at 30% B, linear increase to 90% B over 0.8 min, hold at 90% B for 0.6 min, and a return to 30% B over 0.1 min followed by a re-equilibration (0.5 min) to provide a 2.0 min total run time per sample. HPLC flow

rate was 0.5 mL/min, source temperature was 500 °C, and mass spectral analyses were performed using the following MRM transitions: 353.5 → 259.2 and 353.5 → 123.2 *m/z*. ESI was achieved by a Turbo-Ionspray source in positive ionization mode (5.0 kV spray voltage). The raw plasma and brain concentration data obtained by LC-MS/MS were analyzed by Analyst software (AB Sciex, version 1.5.1), which used the ratio of peak area responses of drug relative to internal standard to construct a standard curve with a dynamic range covering the concentrations found in the samples. Free plasma and brain concentrations were calculated by multiplication of the total concentration values by f_u plasma and f_u brain, respectively, based on data from in vitro rat plasma protein and rat brain homogenate binding experiments.

Rotarod. The effects of **16a** on motor performance were evaluated using an automated rotarod setup with a rotarod (7.0 cm in diameter) rotating at a constant speed of 20 rotations/min (MedAssociates, Inc., St Albans, CA). Male Harlan Sprague–Dawley rats (Harlan Laboratories, Indianapolis, IN) weighing 250–300 g were used. Animals were given two training trials of 120 s on the rotarod with a 10 min interval between trials, followed by baseline assessment of performance with a 120 s trial, any animals that did not reach a performance criteria of 85 s were excluded from the study. Animals were next pretreated for 30 min with vehicle (20% HP- β -CD) or a dose of **16a** ($n = 6$ each group) and then tested on the rotarod using a 120 s trial. The amount of time in s that each animal remained on the rotarod was recorded; animals not falling off of the rotarod were given a maximal score of 120 s. Data were expressed as the mean latency to fall off the rotarod in seconds for each treatment group. **Data Analysis.** Behavioral data were analyzed using a one-way ANOVA with main effects of treatment. Post hoc analyses were performed using a Dunnett's *t* test with all treatment groups compared to the vehicle group using JMP 8.0 (SAS Institute, Cary, NC) statistical software. Data were graphed using SigmaPlot for Windows Version 11.0 (Saugua, MA). A probability of $p \leq 0.05$ was taken as the level of statistical significance.

Modified Irwin Neurological Test Battery. Male Harlan Sprague–Dawley rats (Harlan Laboratories, Indianapolis, IN) weighing 250–300 g were used. Animals were evaluated in the modified Irwin neurological test battery at $t = 0$ to provide a baseline measurement across each functional end point. Animals were next administered either vehicle (20% HP- β -CD) or a 100 mg/kg p.o. dose of **16a** ($n = 6$ each group) and then assessed after a 30 min, 1 h, and 4 h pretreatment interval in the modified Irwin neurological test battery. Changes in the different functional end points of the Irwin test battery were given a score of 0, 1 or 2; with 0 = no effect, 1 = moderate effect, and 2 = robust full effect. All data were collected blinded to treatment for each animal. Following functional end points were scored. Autonomic nervous system functions: ptosis, exophthalmos, miosis, mydriasis, corneal reflex, pinna reflex, piloerection, respiratory rate, writhing, tail erection, lacrimation, salivation, vasodilation, skin color, irritability and rectal temperature; Somatomotor nervous system functions: motor activity, ataxia, arch/roll, tremors, leg weakness, rigid stance, spraddle, placing loss, grasping loss, righting loss, catalepsy, tail pinch reaction, escape loss and physical appearance. **Data Analysis.** Mean change values for each functional end point in the Irwin test battery of each treatment group were calculated using Microsoft Excel. Behavioral data were then analyzed using a one-way ANOVA with main effect of treatment. Post hoc analyses were performed using a Dunnett's *t* test with all treatment groups compared to the vehicle group using JMP 8.0 (SAS Institute, Cary, NC) statistical software. Data were graphed using SigmaPlot for Windows Version 11.0 (Saugua, MA). A probability of $p \leq 0.05$ was taken as the level of statistical significance.

■ ASSOCIATED CONTENT

● Supporting Information

The different LCMS methods used for the characterization of intermediate and final compounds. Mean scores of **16a** effects on autonomic and somatomotor nervous system functions in

rats. This material is available free of charge via the Internet at <http://pubs.acs.org>.

■ AUTHOR INFORMATION

Corresponding Author

*Phone: +34 925 245778. Fax: +34 925 245771. E-mail: jbartolo@its.jnj.com.

Notes

The authors declare no competing financial interest.

■ ACKNOWLEDGMENTS

Vanderbilt Center for Neuroscience Drug Discovery (VCNDD) research was supported by grants from Janssen Pharmaceutical Companies of Johnson & Johnson and in part by the NIH (NS031373, MH062646). The authors would like to thank Dr. Lieve Heylen and Dr. Tom Jacobs for their help with data management and interpretation, Dr. Han Min Tong for her assistance in the preparation of this manuscript, and the members of the purification and analysis group and the biology and ADME/Tox teams from Janssen R&D for their experimental contribution.

■ ABBREVIATIONS USED

AMP, *d*-amphetamine hemisulfate; AUC, area under the curve; b/p, brain to plasma ratio; chromanone, 2,3-dihydro-4*H*-1-benzopyran-4-one; CL_p , plasma clearance; C_{max} , peak plasma concentration; CNS, central nervous system; CRC, concentration response curve; D_2 , dopamine 2; DAD, diode array detector; dihydrobenzothiazolone, 5,6-dihydro-7(4*H*)-benzothiazolone; dihydrothiazolopyridone, 6,7-dihydro-thiazolo[5,4-*c*]pyridin-4(5*H*)-one; DMPK, drug metabolism and pharmacokinetic; E_{hep} , hepatic extraction ratio; EPS, extrapyramidal symptoms; ESCI, electrospray combined with atmospheric pressure chemical ionization; f_w , fraction unbound; GABAergic, γ -aminobutyric acidergic; HEK, human embryonic kidney; HLM, human liver microsome; HP- β -CD, 2-hydroxypropyl- β -cyclodextrin; HPLC, high-performance liquid chromatography; HTS, high throughput screening; iv, intravenous; LC-HRMS, liquid chromatography combined with high resolution mass spectrometry; LCMS, liquid chromatography combined with mass spectrometry; LE, ligand efficiency; M_p , melting point; NMDA, *N*-methyl-D-aspartate; mGlu, metabotropic glutamate; NMR, nuclear magnetic resonance (NMR); mGlu₅, metabotropic glutamate 5; PAM, positive allosteric modulator; PK, pharmacokinetic; PKC, protein kinase C; ppm, parts per million; p.o., oral; RLM, rat liver microsome; RP-HPLC, reversed-phase high-performance liquid chromatography; SAR, structure activity relationship; sc, subcutaneous; SPR, structure properties relationship; $T_{1/2}$, half-life; T_{max} , t_R , retention time; time to reach peak concentration; TLC, thin layer chromatography; VCNDD, Vanderbilt Center for Neuroscience Drug Discovery

■ REFERENCES

- (1) Tandon, R.; Nasrallah, H. A.; Keshavan, M. S. Schizophrenia, "Just the Facts" 4. Clinical Features and Conceptualization. *Schizophr. Res.* **2009**, *110*, 1–23.
- (2) Conn, P. J.; Lindsley, C. W.; Jones, C. K. Activation of Metabotropic Glutamate Receptors as a Novel Approach for the Treatment of Schizophrenia. *Trends Pharmacol. Sci.* **2009**, *30*, 148–155.

- (3) Macdonald, G. J.; Bartolome, J. M. A Decade of Progress in the Discovery and Development of 'Atypical' Antipsychotics. *Prog. Med. Chem.* **2010**, *49*, 37–80.
- (4) Olney, J. W.; Farber, N. B. NMDA Antagonists as Neurotherapeutic Drugs, Psychotogens, Neurotoxins, and Research Tools for Studying Schizophrenia. *Arch. Gen. Psychiatry* **1995**, *52*, 998–1007.
- (5) Nakanishi, S. Molecular Diversity of Glutamate Receptors and Implications for Brain Functions. *Science* **1992**, *258*, 597–603.
- (6) Shigemoto, R.; Mizuno, N. Metabotropic Glutamate Receptors – Immunocytochemical and In Situ Hybridization Analysis. In *Handbook of Chemical Neuroanatomy*; Ottersen, O. P.; Storm-Mathisen, J., Eds.; Elsevier: Amsterdam, 2000; pp 63–98.
- (7) Cauli, B.; Porter, J. T.; Tsuzuki, K.; Lambolez, B.; Rossier, J.; Quenet, B.; Audinat, E. Classification of Fusiform Neocortical Interneurons Based on Unsupervised Clustering. *Proc. Natl. Acad. Sci. U. S. A.* **2000**, *97*, 6144–6149.
- (8) Perroy, J.; Raynaud, F.; Homburger, V.; Rousset, M.-C.; Telley, L.; Bockaert, J.; Fagni, L. Direct Interaction Enables Cross-talk between Ionotropic and Group I Metabotropic Glutamate Receptors. *J. Biol. Chem.* **2008**, *283*, 6799–6805.
- (9) Stauffer, S. R. Progress toward Positive Allosteric Modulators of the Metabotropic Glutamate Receptor Subtype 5 (mGluR5). *ACS Chem. Neurosci.* **2011**, *2*, 450–470.
- (10) Lindsley, C. W.; Wisnoski, D. D.; Leister, W. H.; O'Brien, J. A.; Lemiere, W.; Williams, D. L., Jr.; Burno, M.; Sur, C.; Kinney, G. G.; Pettibone, D. J.; Miller, P. R.; Smith, S.; Duggan, M. E.; Hartman, G. D.; Conn, P. J.; Huff, J. R. Discovery of Positive Allosteric Modulators for the Metabotropic Glutamate Receptor Subtype 5 from a Series of N-(1,3-Diphenyl-1H-pyrazol-5-yl)benzamides That Potentiate Receptor Function In Vivo. *J. Med. Chem.* **2004**, *47*, 5825–5828.
- (11) Kinney, G. G.; O'Brien, J. A.; Lemaire, W.; Burno, M.; Bickel, D. J.; Clements, M. K.; Wisnoski, D. D.; Lindsley, C. W.; Tiller, P. R.; Smith, S.; Jacobson, M. A.; Sur, C.; Duggan, M. E.; Pettibone, D. J.; Williams, D. W., Jr. A Novel Selective Positive Allosteric Modulator of Metabotropic Glutamate Receptor Subtype 5 Has In Vivo Activity and Antipsychotic-like Effects in Rat Behavioral Models. *J. Pharmacol. Exp. Ther.* **2005**, *313*, 199–206.
- (12) Liu, F.; Grauer, S.; Kelley, C.; Navarra, R.; Graf, R.; Zhang, G.; Atkinson, P. J.; Popiolek, M.; Wantuch, C.; Khawaja, X.; Smith, D.; Olsen, M.; Kouranova, E.; Lai, M.; Pruthi, F.; Pulicchio, C.; Day, M.; Gilbert, A.; Pausch, M. H.; Brandon, N. J.; Beyer, C. E.; Comery, T. A.; Logue, S.; Rosenzweig-Lipson, S.; Marquis, K. L. ADX47273 [S-(4-Fluoro-phenyl)-{3-[3-(4-fluoro-phenyl)-[1,2,4]oxadiazol-5-yl]-piperidin-1-yl}-methanone]: A Novel Metabotropic Glutamate Receptor 5-Selective Positive Allosteric Modulator with Preclinical Antipsychotic-like and Procognitive Activities. *J. Pharmacol. Exp. Ther.* **2008**, *327*, 827–839.
- (13) Rodriguez, A. L.; Grier, M. D.; Jones, C. K.; Herman, E. J.; Kane, A. S.; Smith, R. L.; Williams, R.; Zhou, Y.; Marlo, J. E.; Days, E. L.; Blatt, T. N.; Jadhav, S.; Menon, U.; Vinson, P. N.; Rook, J. M.; Stauffer, S. R.; Niswender, C. M.; Lindsley, C. W.; Weaver, C. D.; Conn, P. J. Discovery of Novel Allosteric Modulators of Metabotropic Glutamate Receptor Subtype 5 Reveals Chemical and Functional Diversity and In Vivo Activity in Rat Behavioral Models of Anxiolytic and Antipsychotic Activity. *Mol. Pharmacol.* **2010**, *78*, 1105–1123.
- (14) (a) Gastambide, F.; Cotel, M. C.; Gilmour, G.; O'Neill, M. J.; Robbins, T. W.; Tricklebank, M. D. Selective Remediation of Reversal Learning Deficits in the Neurodevelopmental MAM Model of Schizophrenia by a Novel mGlu₅ Positive Allosteric Modulator. *Neuropsychopharmacology* **2012**, *37*, 1057–1066. (b) Gastambide, F.; Gilmour, G.; Robbins, T. W.; Tricklebank, M. D. The mGlu₅ Positive Allosteric Modulator LSN2463359 Differentially Modulates Motor, Instrumental and Cognitive Effects of NMDA Receptor Antagonists in the Rat. *Neuropharmacology* **2013**, *64*, 240–247.
- (15) Gilmour, G.; Broad, L. M.; Wafford, K. A.; Britton, T.; Colvin, E. M.; Fivush, A.; Gastambide, F.; Getman, B.; Heinz, B. A.; McCarthy, A. P.; Prieto, L.; Shanks, E.; Smith, J. W.; Taboada, L.; Edgard, D. M.; Tricklebank, M. D. In Vitro Characterisation of the Novel Positive Allosteric Modulators of the mGlu₅ Receptor, LSN2463359 and LSN2814617, and Their Effects on Sleep architecture and Operant Responding in the Rat. *Neuropharmacology* **2013**, *64*, 224–239.
- (16) Hammond, A. S.; Rodriguez, A. L.; Townsend, S. D.; Niswender, C. M.; Jones, C. K.; Lindsley, C. W.; Conn, P. J. Discovery of a Novel Chemical Class of mGlu₅ Allosteric Ligands with Distinct Modes of Pharmacology. *ACS Chem. Neurosci.* **2010**, *1*, 702–716.
- (17) Zhou, Y.; Manka, J.; Rodriguez, A. L.; Weaver, C. D.; Jones, C. K.; Conn, P. J.; Lindsley, C. W.; Stauffer, S. R. Discovery of N-Aryl Piperazines as Selective mGluR5 Potentiators with Improved In Vivo Utility. *ACS Med. Chem. Lett.* **2010**, *1*, 433–438.
- (18) Spear, N.; Gadiant, R. A.; Wilkins, D. E.; Do, M. L.; Smith, J. S.; Zeller, K. L.; Schroeder, P.; Zhang, M.; Arora, J.; Chhajlani, V. Preclinical Profile of a Novel Metabotropic Glutamate Receptor 5 Positive Allosteric Modulator. *Eur. J. Pharmacol.* **2011**, *659*, 146–154.
- (19) Chromanone derivatives **9**, **10**, **11** and **12** have recently also been described as mGlu₅ receptor PAMs by Varnes *et al.* confirming our findings. Varnes, J. G.; Marcus, A. P.; Mauger, R. C.; Throner, S. R.; Hoesch, V.; King, M. M.; Wang, X.; Sygowski, L. A.; Spear, N.; Gadiant, R.; Brown, D. G.; Campbell, J. B. Discovery of Novel Positive Allosteric Modulators of the Metabotropic Glutamate Receptor 5 (mGlu₅). *Bioorg. Med. Chem. Lett.* **2011**, *21*, 1402–1406.
- (20) Compounds were tested for agonist, PAM, or antagonist activity on mGlu receptors in fluorescent Ca²⁺ assays using HEK293 cells expressing human mGlu₁, mGlu₂, mGlu₃, mGlu₇, or mGlu₈ receptors. Effects on the human mGlu₄ receptor were tested in Ca²⁺ or [³⁵S]-GTPγS functional assays (receptor either expressed in HEK293 or L929sA cells). Evaluation of effects on the rat mGlu₆ receptors expressed in CHO cells were assessed in [³⁵S]-GTPγS functional assays.
- (21) Hopkins, A. L.; Groom, C. R.; Alex, A. Ligand Efficiency: a Useful Metric for Lead Selection. *Drug Discovery Today* **2004**, *9*, 430–431.
- (22) Data not shown.
- (23) Manka, J. T.; Vinson, P. N.; Gregory, K. J.; Zhou, Y.; Williams, R.; Gogi, K.; Days, E.; Jadhav, S.; Herman, E. J.; Lavreysen, H.; Mackie, C.; Bartolomé, J. M.; Macdonald, G. J.; Steckler, T.; Daniels, J. S.; Weaver, C. D.; Niswender, C. M.; Jones, C. K.; Conn, P. J.; Lindsley, C. W.; Stauffer, S. R. Optimization of an Ether Series of mGlu₅ Positive Allosteric Modulators: Molecular Determinants of MPEP-site Interaction Crossover. *Bioorg. Med. Chem. Lett.* **2012**, *22*, 6481–6485.
- (24) Macdonald, G. J.; Tresadern, G. J.; Trabanco-Suarez, A. A.; Pastor-Fernandez, J. Preparation of Bicyclic Thiazoles as Allosteric Modulators of mGluR5 Receptors. WO 2011073347 A1, 2011.
- (25) Macdonald, G. J.; Trabanco-Suarez, A. A.; Conde-Ceide, S.; Tresadern, G. J.; Bartolome-Nebreda, J. M.; Pastor-Fernandez, J. Preparation of Bicyclic Thiazoles as Allosteric Modulators of mGluR5 Receptors. WO 2011073339 A1, 2011.
- (26) Brandl, T.; Maier, U.; Hoffmann, M.; Scheuerer, S.; Joergensen, A. T.; Pautsch, A.; Breitfelder, S.; Grauert, M.; Hoenke, C.; Erb, K.; Pieper, M.; Pragst, I. Preparation of Dihydrothiazoloquinazolines as PI-3 Kinase Inhibitors. WO 2007115929 A1, 2007.
- (27) Noetzel, M. J.; Rook, J. M.; Vinson, P. N.; Cho, H. P.; Days, E.; Zhou, Y.; Rodriguez, A. L.; Lavreysen, H.; Stauffer, S. R.; Niswender, C. M.; Xiang, Z.; Daniels, J. S.; Lindsley, C. W.; Weaver, C. D.; Conn, P. J. Functional Impact of Allosteric Agonist Activity of Selective Positive Allosteric Modulators of Metabotropic Glutamate Receptor Subtype 5 in Regulating Central Nervous System Function. *Mol. Pharmacol.* **2012**, *81*, 120–133.
- (28) LeadProfilingScreen. Ricerca Biosciences. Screen performed on the following targets: A₁, A_{2A}, A₃, α_{1A}, α_{1B}, α_{1D}, α_{2A}, β₁, β₂, AR, B₁, B₂, CaCH L-Type (benzothiazepine), CaCH L-Type (dihydropyridine), CaCH N-Type, CB₁, D₁, D_{2S}, D₃, D_{4.2}, ET_A, ET_B, EGF, ER_α, GABA_A (flunitrazepam), GABA_A (muscicoline), GABA_{B1A}, GR, kainate, NMDA (agonism), NMDA (glycine), NMDA (phencyclidine), H₁, H₂, H₃, IL-1, CysLT₁, MT₁, M₁, M₂, M₃, NPY₁, NPY₂, acetylcholine, acetylcholine α₁ (bungarotoxin), OP₁, OP₂, OP₃, phorbol ester, PAF, KCH_{ATP},

hERG, EP₄, P_{2X}, P_{2Y}, rolipram, 5HT_{1A}, 5HT_{2B}, 5HT₃, σ_1 , NK₁, thyroid hormone, DAT, GABA transporter, NET, SERT.

(29) Gregory, K. J.; Noetzel, M. J.; Rook, J. M.; Vinson, P. N.; Stauffer, S. R.; Rodriguez, A. L.; Emmitte, K. A.; Zhou, Y.; Chun, A. C.; Felts, A. S.; Chauder, B. A.; Lindsley, C. W.; Niswender, C. M.; Conn, P. J. Investigating Metabotropic Glutamate Receptor 5 Allosteric Modulator Cooperativity, Affinity and Agonism: Enriching Structure-function Relationships. *Mol. Pharmacol.* **2012**, *82*, 860–875.

(30) Based upon rat brain homogenate binding fraction unbound (18%) and total brain levels ($[\text{brain}]_{90\text{min}} = 17.5 \pm 13.4 \mu\text{M}$). Estimated average terminal unbound brain concentrations of **16a** after the 3, 10, 30, and 56.6 p.o. doses were 14 ± 11 , 15 ± 13 , 551 ± 449 , and 908 ± 1029 nM respectively.

(31) Carter, R. J.; Morton, J.; Dunnett, S. B. Motor Coordination and Balance in Rodents. *Curr. Protocols Neurosci.* **2001**, 8.12.1–8.12.14.

(32) Measures included scoring for ptosis, exophthalmos, miosis, mydriasis, corneal reflex, pinna reflex, piloerection, respiratory rate, writhing, tail erection, lacrimation, salivation, vasodilation, skin color, irritability, rectal temperature, motor activity, ataxia, arch/roll, tremors, leg weakness, rigid stance, spraddle, placing loss, grasping loss, righting loss, catalepsy, tail pinch reaction, escape loss and physical appearance.